Ultrafast vibrational spectroscopy in condensed phases

Minhaeng Cho

Department of Chemistry and Center for Multidimensional Spectroscopy, Korea University, Seoul 136-701, Korea. E-mail: mcho@korea.ac.kr

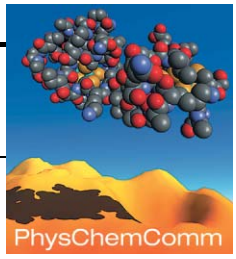

Perspective

Received 28th November 2001, Accepted 8th February 2002
Published on the Web 21st February 2002

A variety of ultrafast vibrational excitation and probing methods are first discussed and it is shown that various vibrational spectroscopies can be devised by combining multiple excitation and probing methods. A few ultrafast vibrational spectroscopic methods in condensed phases, which have already been demonstrated and used to study vibrational relaxation phenomena and structural analysis of small polypeptides, are briefly summarized. Then, a number of novel ultrafast vibrational spectroscopies that have been theoretically investigated are discussed by emphasizing their differences from other existing methods. Perspectives on how these ultrafast vibrational spectroscopies in centrosymmetric and non-centrosymmetric condensed phases can be applied to the investigations of chemical reaction dynamics, solvation dynamics, time-dependent structural evolutions of polyatomic molecules such as proteins will be mentioned.

I. Introduction

Ultrafast laser spectroscopy in condensed phases has been extensively used to study sub-picosecond solvation dynamics, chemical reactions, semiconductor dynamics, and biological reactions. Due to the advent of the laser technology, femtosecond laser system operating in the visible frequency range has been commercially available so that the range of applications utilizing ultrafast nonlinear spectroscopic methods has been and will be expanding greatly. Recently, the ultrafast vibrational dynamics has received much attention both because there was an advancement in developing a stable coherent infrared laser sources and because the width of femtosecond optical laser pulses is short now enough (or spectrally broad enough) to excite intramolecular vibrational degrees of freedom impulsively.[1,2] There already exist review articles on the time-resolved vibrational spectroscopy including the seminal review paper by Laubereau and Kaiser in 1978.[3–5] The goal of this perspectives article is not simply to review current research results in the field of ultrafast vibrational spectroscopy in condensed phases. Therefore, the excitation and probing methods typically used in the ultrafast vibrational spectroscopy will be briefly outlined and a number of theoretically proposed vibrational spectroscopic methods will be discussed more in detail instead. Also, perspectives and interesting applications of the ultrafast multidimensional vibrational spectroscopy will be discussed in the present paper.

Over the last two decades, the main concerns of the ultrafast vibrational spectroscopy have been the vibrational dephasing and intra- and intermolecular vibrational population relaxation processes in condensed phases.[3,4,6–16] These phenomena are crucial in understanding physical and chemical processes in condensed phases.[17–20] For example, intra- and intermolecular vibrational energy relaxation is the key to understanding the chemical reaction dynamics in solution. During each event of a chemical reaction, one or more transition states that are energetically unstable are created and the excess energy has to be eventually dissipated into the other intramolecular and solvent degrees of freedom. Thus, the theoretical description of the chemical reaction dynamics in condensed phases has to rely on vibrational energy relaxation processes. In order to measure the vibrational relaxation from a specific vibrationally excited state to the bath degrees of freedom, IR pump–probe spectroscopy has been used.[3,21–34] Also, ultrafast IR-Raman spectroscopy, which was initially discussed by Kaiser and Laubereau,[3] was found to be exceptionally useful in studying vibrational population redistribution among different vibrational states.[35–48] In parallel with these investigations on the vibrational energy relaxation, the IR photon echo method has been used to specifically measure the homogeneous vibrational dephasing rate by measuring the IR echo field generated by the rephasing process in an inhomogeneously broadened system.[49–59] Although there exist a number of experimental results related to the vibrational dephasing and energy relaxation rates, theoretical predictions of the vibrational relaxation rates have been partly successful.

Although the main goal of the ultrafast vibrational spectroscopy in the past has been the elucidation of the vibrational relaxation processes, the focus of future investigations will shift to the direct investigation of the vibrational coupling mechanisms (Fig. 1). Over the last few years, numerous multidimensional vibrational spectroscopies have been used and the number of publications in this research field increased dramatically.[1,2,5,48,55–96] The main advantage of these multidimensional vibrational spectroscopies is that they are capable of extracting quantitative information on the vibrational couplings induced by electric and mechanical anharmonicities of the vibrational chromophores in condensed phases. For example, the applications of IR pump–probe spectroscopy to amide I vibrations of polypeptides provide information on the mechanical anharmonicity-induced frequency shift, which is a sensitive function of the three-dimensional structure of a given polypeptide.[33,34] The fifth-order Raman scattering

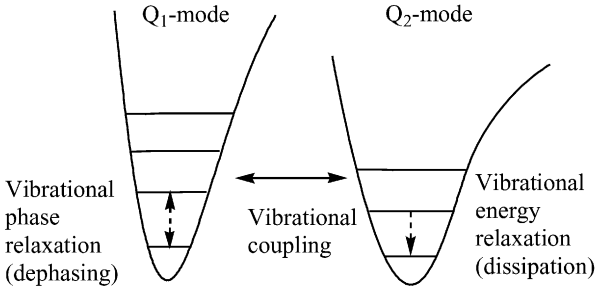

Fig. 1 Various vibrational coupling and relaxation mechanisms.

measurement revealed the mode–mode coupling patterns in the intermolecular vibrational degrees of freedom of liquids.[5,60,65,97–102] Thus, the future applications of ultrafast multidimensional vibrational spectroscopy will be to obtain the vibrational coupling map of a complicated molecular system.[73] Of course, the quantitative determination of the vibrational coupling mechanisms will be of effective use in the description of the vibrational energy relaxation in a given molecule. However, the main focus will still be to establish the 3D structure–vibrational coupling relationships. To be more specific, let's consider the multidimensional potential energy surface that can be expanded as

$$V(\{Q_j\}) = V_0 + \frac{1}{2}\sum_j m_j\omega_j^2 Q_j^2 + \frac{1}{3!}\sum_{i,j,k}\left(\frac{\partial^3 V}{\partial Q_i \partial Q_j \partial Q_k}\right) Q_i Q_j Q_k + \frac{1}{4!}\sum_{i,j,k,l}\left(\frac{\partial^4 V}{\partial Q_i \partial Q_j \partial Q_k \partial Q_l}\right) Q_i Q_j Q_k Q_l + \cdots \quad (1)$$

The one-dimensional vibrational spectra, such as IR absorption and Raman scattering spectra, provide information on the distribution of the vibrational modes, which are mainly determined by the quadratic part of the potential function. The fundamental transition frequencies are slightly different from ω_j due to the anharmonic terms. Nevertheless, the major information that can be extracted from the one-dimensional vibrational spectra is whether a certain functional group exists in a given molecule or not. Thus, the 1D spectrum provides a list of functional groups included in the target molecule, *i.e.*, O–H, C=C, C=O, N–H *etc.* However, the vibrational couplings among these different functional groups cannot be easily studied if the size of the molecule increases, because the combination and overtone band intensities are very weak and they are often hidden under the intense fundamental peaks or solvent peaks. Unlike the dominant quadratic (harmonic) part of the potential function, the cubic and quartic anharmonic coefficients are likely to be very sensitive with respect to the actual 3D molecular structure. Thus, multidimensional vibrational spectroscopy utilizing multiple pulses will be of crucial use in quantitatively determining the vibrational coupling patterns.

In relation to this statement, it is interesting to note the analogy depicted in Fig. 2. Let's consider the structural analysis of a given protein. The first and most important step is to delineate the primary sequence of the amino acids of the protein under investigation. If one measures the entire 1D vibrational spectrum (particularly the fingerprint region), it will directly tell us about what functional groups are included in the protein. This information can be easily inferred by inspecting the primary sequence of the protein, *e.g.*, O–H peak from Tyr, N–H and C=O peaks from peptides, COOH peak from Glu, *etc.* However, the 1D spectrum will not provide sufficiently detailed information on the secondary or tertiary structures, even though there are a number of empirical rules used to predict the existence of α-helix or β-sheet (for example, the detailed shape of the amide I vibrational band in an IR spectrum is weakly dependent on the secondary structures).[103–105] Thus, one requires a larger number of observables that can be used to determine the 3D structure of the protein. This is basically why 2D or 3D NMR is advantageous in comparison to the 1D NMR.[106,107] The 2D NMR spectra contain many more peaks and thus the one-to-one correspondence between the 2D NMR spectrum and the 3D protein structure can further be ensured. Thus, as depicted in Fig. 2, the 1D NMR and 1D vibrational spectroscopies are methods which measure *large* or dominant quantities, whereas the multidimensional NMR and vibrational spectroscopies are designed to measure *small* quantities which cannot be easily obtained with the corresponding 1D methods. Here it should be emphasized that the latter issue is not one of frequency-resolution. Even if one has an ultra-high resolution method, the intrinsic limit of the 1D method still exists and cannot be overcome by simply increasing the frequency-resolution. Now, the cubic and quartic anharmonicities in the potential surface are likely to be small near the bottom of the potential energy surface. For example, the 2D and 3D vibrational spectra, which are sensitively dependent on these small quantities, *i.e.*, the mechanical and electric anharmonicities, will be much more strongly dependent on the secondary and tertiary structures of proteins. This is why the measurement of the small quantities is crucial in the structure determination of the polyatomic molecules. The advantages of 2D and 3D vibrational spectroscopy in comparison with 1D spectroscopy will be discussed in Section IV in more detail.

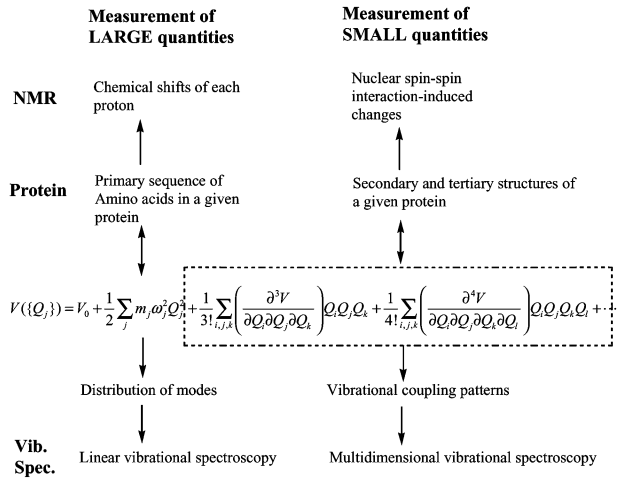

Fig. 2 Analogy between NMR and vibrational spectroscopy.

This paper is organized as following. Ultrafast vibrational excitation and probing methods are outlined in Section II. The general theory on the linear and nonlinear response functions, which are associated with all the ultrafast vibrational spectroscopies discussed in this paper, will be summarized in Section III. Various ultrafast vibrational spectroscopies that have been applied to centrosymmetric and non-centrosymmetric systems will be briefly discussed in Sections V and VI. Novel vibrational spectroscopies that have not been experimentally realized and experimental perspectives will be summarized in Section VII. A number of future applications of the ultrafast vibrational spectroscopy will be proposed in Section VIII.

II. Ultrafast vibrational excitation and probing methods

In order to classify each different ultrafast vibrational spectroscopy, it is necessary to summarize the vibrational excitation and probing methods first.

A. Ultrafast vibrational excitation methods

There are numerous time-domain methods to vibrationally excite molecules in condensed phases. Depending on the properties in which experimentalists are interested, one can probe the relaxation of the diagonal (population state) or off-diagonal (vibrational coherent state) density matrix elements. Thus, the ultrafast excitation methods are mainly divided into two classes. The first is to vibrationally excite a molecule to create non-equilibrium population distribution, whereas the

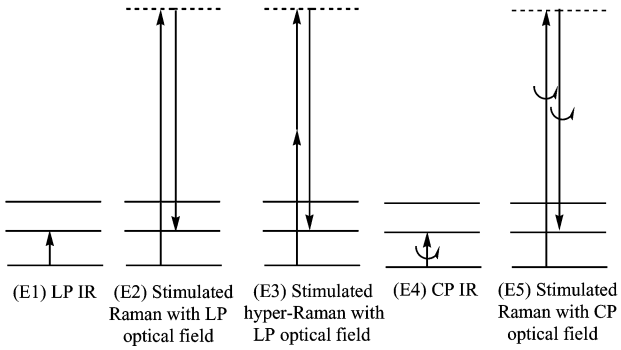

Fig. 3 Five representative vibrational excitation methods. The horizontal lines are the vibrational quantum states on the electronic ground state. The dashed horizontal line corresponds to the virtual state involved in the Raman or hyper-Raman transitions. The methods (E4) and (E5) involve circularly polarized IR or optical fields.

second is to create a vibrational coherence state. Since the former involves population relaxation and the latter involves vibrational phase relaxation, we shall denote Epop and Epha for the two distinct excitation schemes. In any case, the five representative excitation methods that will be considered in this article are (see Fig. 3)

(E1) Resonant infrared pulse

(E2) Stimulated Raman excitation with electronically off-resonant optical pulse

(E3) Stimulated hyper-Raman excitations

(E4) Resonant infrared excitation with circularly polarized light

(E5) Stimulated Raman excitation with circularly polarized light *etc.*

Vibrational coherence state generation. The first and most straightforward method (Epha1) is to use a resonant infrared pulse to selectively excite a specific vibrational degree of freedom. Since the IR-field–matter interaction is given as $-\mu E(t)$, the force exerted on the jth vibrational degree of freedom is $(\partial\mu/\partial Q_j)E(t)$. The dipole moment is denoted by μ. Now, due to the finite spectral width of a sub-picosecond IR pulse $\tilde{E}(\omega)$, which is determined by the Fourier-transform of the temporal IR-pulse envelope function, the excitation process inevitably involves a range of vibrational excitations arising from frequencies that are within the envelope of the pulse spectrum, $\tilde{E}(\omega)$. This aspect is, however, useful since the excitation of multiple vibrational degrees of freedom in the vibrational excitonic manifold results in a broad dispersed signal spectrum revealing vibrational interactions. The second method (Epha2) is to use the stimulated Raman process to vibrationally excite molecules. By using an ultrafast optical pulse whose frequency is far off-resonant with respect to the electronic transition, the Raman-active vibrational modes can be excited when the corresponding vibrational frequencies are within the spectral width of the short pulse. In this case, the effective field–matter interaction is $-\alpha|E(t)|^2$, where the polarizability is denoted as α, so that the force exerted on the jth vibrational degree of freedom is $(\partial\alpha/\partial Q_j)|E(t)|^2$. For example, the third-order optical Kerr measurement (or impulsive stimulated Raman scattering experiment) involves almost impulsive vibrational excitation with an ultrafast optical pulse ($|E(t)|^2 \sim E_0^2\delta(t)$). The third method (Epha3) involves a higher-order field–matter interaction, hyper-Raman process, so that the effective field–matter interaction in this case is $-\beta E_1(t)E_2(t)E_3^*(t)$, where β is the first hyperpolarizability and the three injected fields are denoted as $E_j(t)$. Then, the jth mode will experience the force, $(\partial\beta/\partial Q_j)E_1(t)E_2(t)E_3^*(t)$, when the molecule is exposed to the three electronically off-resonant fields. Often, the vibrational selection rule of the hyper-Raman process differs from that of the Raman process so that the stimulated hyper-Raman excitation method will excite different vibrational degrees of freedom in comparison to the conventional impulsive Raman scattering method.

So far, cases where the injected external fields are linearly polarized (LP) were considered. However, there will be a completely new set of vibrational excitation schemes if the IR and optical fields are circularly polarized (CP). As recently proposed by the author,[108] a time-resolved vibrational optical activity measurement can be achieved by using CP light beams. The only experimental scheme discussed in ref. 108 is the infrared–visible sum–frequency–generation spectroscopy for an isotropic system with chiral molecules. The methods (Epha4) and (Epha5) use CP IR or CP optical fields to vibrationally excite the target molecules. As will be discussed later in this paper, a vibrational optical activity measurement in the time domain will provide critical information on the structural evolution of chiral molecules, such as protein folding process in solution.

Vibrational population state generation. By using the five excitation methods in Fig. 3, one can also create vibrational populations on the excited states. The first method (Epop1) involves two IR-field-matter interactions, *i.e.*, one-photon annihilation, to create a new population on the vibrationally excited state. Similarly, Epop2, Epop3, Epop4, and Epop5 methods can be used to build up population on the vibrationally excited state. Then, the population relaxation processes can be probed by using the ultrafast probing methods denoted as Ppop1 ~ Ppop3 discussed in the following subsection.

B. Ultrafast probing methods

After the vibrational excitation using one of the methods outlined in the previous section, the dynamics of the perturbed quantum system can be probed in time. In general, there are two classes of probing methods. The first is to measure the population changes of a given vibrational state, *i.e.*, time evolution of the diagonal density matrix. The second is to measure the relaxation of the vibrational coherence state, *i.e.*, time evolution of the off-diagonal density matrix. The former class of probing methods will be denoted as "Ppop", where Ppop stands for Probing population relaxation, whereas the latter types of probing methods will be denoted as "Ppha", where Ppha means Probing phase relaxation. Here it should be noted that the relaxation of the off-diagonal density matrix is determined by both the pure dephasing and the population relaxation rates.

First, let's consider the Ppop methods. Once a non-equilibrium population distribution is created by the field–matter interaction using one of the excitation methods in Section II-A, one can use one of the following methods to probe the time-dependent relaxation of the diagonal density matrix;

(Ppop1) IR probe absorption

(Ppop2) Incoherent Raman scattering

(Ppop3) Coherent Raman scattering, *etc.*

The first method (Ppop1) is to use an IR probe pulse and measure the IR probe absorption, which is determined by the excitation from the first excited state to the second excited state as well as by the photo-bleaching recovery. The simplest experiment using the Ppop1 method is the IR pump–probe spectroscopy.[3,21–34] The second method (Ppop2) is to use an electronically off-resonant optical pulse and measure the incoherent *anti*-Stokes or Stokes Raman scattering spectrum.[3] The ultrafast IR-Raman method is just one example using the Ppop2 detection scheme. In this case, the IR pump pulse selectively excites a vibrational mode so that the diagonal

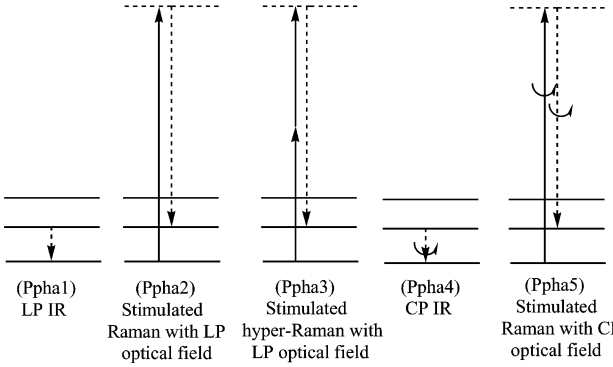

Fig. 4 The upward solid arrow represents the transitions induced by the external-field-matter interactions, whereas the downward dashed arrow is the spontaneously emitted field-matter interaction. The probing methods (Ppha4) and (Ppha5) detect the circularly polarized signal field.

density matrix differs from the thermal equilibrium density matrix. Then, the vibrational population is redistributed to other coupled modes and the population of each different vibrational state can be time-resolved by measuring the incoherent Raman spectrum after the time-delayed off-resonant optical pulse. The third method (Ppop3) for the detection of the diagonal density matrix evolution is to use the coherent Raman scattering process. Although third-order coherent Raman scattering, such as the optical Kerr measurement or impulsive stimulated Raman scattering,[109–120] has been extensively used to study ultrafast liquid dynamics, the initial state was nothing but a thermally equilibrium state. However, one can use an intense IR pulse to build up a population on a particular vibrational state. Then, the coherent Raman scattering method can be applied to this non-equilibrium state to measure the vibrational population redistribution in liquids. This method, the so called IR-optical Kerr effect (IR-OKE) measurement[121] was theoretically proposed by the author and will be discussed in Section VII in more detail.

We next discuss various probing methods that are particularly useful in measuring the off-diagonal density matrix evolution. Much like the ultrafast excitation processes, one can use the same types of coherent transition processes. In Fig. 4, the energy level diagrams associated with the five Ppha methods are shown.

The first method (Ppha1) is to measure the polarization of the vibrational coherence state so that the signal field is in the IR frequency range. The Ppha2 method uses the stimulated Raman scattering process. Suppose that a vibrational coherence state, *i.e.*, vibrational transient grating (TG), which is represented by a specific off-diagonal density matrix element, is created by prior field–matter interactions. Then, an electronically off-resonant optical pulse is injected, the vibrational TG can scatter the off-resonant pulse and the measured signal intensity contains information on the evolution of the vibrational coherence state. The third method (Ppha3) is a simple extension of the stimulated Raman scattering method to higher-order (hyper-Raman) scattering process. The other two methods, Ppha4 and Ppha5, are self-evident.

C. Multiple vibrational excitation methods: 1. two-dimensional transient grating generation

In the previous subsection II-A, regardless of the actual excitation methods, after the proper field–matter interaction (or interactions) either one-dimensional vibrational transient grating (TG) or excited state population are created. Depending on the probing method combined with the excitation method, one can measure the population relaxation and/or vibrational dephasing processes. Suppose that one focuses on the case of coherent vibrational spectroscopy measuring relaxation of the vibrational coherence state. If only one vibrational degree of freedom is considered, the relaxation of the vibrational TG is approximately given as $e^{-\gamma_j t}\sin\omega_j t$. After a finite delay time, the transient dynamics of the 1D grating can be measured by using one of the time-domain probing methods, Ppha, discussed in Section II-C. By combining two or more excitation pulses that are separated in time, it is possible to create temporally (and spatially) multidimensional vibrational TG's. Unlike the 1D TG, the signal field generated by the scattering of the probe field from the multidimensional TG is produced by the interference between fields scattered by different nonlinear optical transition pathways.[73]

Then, the number of the different ways to create 2D vibrational TG's is simply the number of combinations of the ultrafast excitation methods outlined in Fig. 3. If only the first three methods are considered, there are 9 distinctly different ways to create a 2D vibrational TG (see Table 1). The perturbed part of the density operators are given in Table 1. One example of the coherent 2D vibrational spectroscopy is the time-resolved fifth-order 2D Raman scattering process,[60–73] which is a time-domain analogue of the CHORES (coherent higher-order Raman emission spectroscopy), which was studied for the first time by Bloembergen and coworkers.[122,123] In this case, the 2D vibrational TG is created by the two stimulated Raman scattering processes, and then the probing method is to detect an additional stimulated Raman scattering field, *i.e.*, Stimulated Raman (Epha2) → Stimulated Raman (Epha2) → Stimulated Raman (Ppha2). Despite that the fifth-order 2D Raman method has suffered from an unexpected complication associated with the cascading process,[124–129] it has the advantage that an optical pulse of a few femtoseconds is short enough to excite a broad range of vibrational modes, in comparison to the IR pulse. Other methods utilizing two tunable IR pulses for the creation of the 2D vibrational TG and one optical pulse, such as IR–IR–Vis sum- and difference-frequency-generation spectroscopies, are also examples of ultrafast 2D vibrational spectroscopy.[73,84,85,89–91,130,131] These IR-Vis four-wave-mixing spectroscopies, which involve a sequence of excitation-probing steps, Epha1–Epha1–Ppha2, have recently been used to study vibrational interactions of acetonitrile and CO adsorbed on a Ru metal surface.[91]

D. Multiple vibrational excitation methods: 2. three-dimensional vibrational transient grating generation

As a natural extension of 1D and 2D vibrational spectroscopies, a number of 3D vibrational spectroscopies can be proposed.[96] If the vibrational chromophores are excited by applying any combination of the three excitation methods and

Table 1 The first and second vibrational excitation processes are listed in the first row and first column, respectively. The thermal equilibrium density operator is denoted as ρ_{eq}, and the perturbed density operators are given in this table

	Resonant IR (μ)	Stimulated Raman (α)	Stimulated hyper-Raman (β)
Resonant IR (μ)	$[\mu(t_2), [\mu(t_1), \rho_{eq}]]$	$[\mu(t_2), [\alpha(t_1), \rho_{eq}]]$	$[\mu(t_2), [\beta(t_1), \rho_{eq}]]$
Stimulated Raman (α)	$[\alpha(t_2), [\mu(t_1), \rho_{eq}]]$	$[\alpha(t_2), [\alpha(t_1), \rho_{eq}]]$	$[\alpha(t_2), [\beta(t_1), \rho_{eq}]]$
Stimulated hyper-Raman (β)	$[\beta(t_2), [\mu(t_1), \rho_{eq}]]$	$[\beta(t_2), [\alpha(t_1), \rho_{eq}]]$	$[\beta(t_2), [\beta(t_1), \rho_{eq}]]$

if only the first three methods in Fig. 3 are considered, there are 27 different ways to create a 3D vibrational TG.

For example, the degenerate IR photon echo experiment generally involves three or four IR pulses that are separated in time, *i.e.*, Epha1–Epha1–Epha1–Ppha1. The final IR pulse in the case of four-pulse IR photon echo experiment is just used as a time-gating pulse. The IR photon echo belongs to the case of 3D vibrational TG experiment in general.[132] In sections V and VII, several 3D vibrational spectroscopies will be discussed in detail.

III. Linear and nonlinear response functions

In sections V and VI a number of different ultrafast vibrational spectroscopies will be discussed and they differ from each other by the combination of excitation and probing methods. Thus, one can choose a specific experimental scheme to investigate particular vibrational dynamics and associated phenomena. Nevertheless, the measured signal can always be written in terms of the corresponding linear and nonlinear response functions. If we restrict our discussion up to 3D vibrational spectroscopy, regardless of the involvement of an electronic resonance phenomenon, there are only three classes of response functions,

$$R_{1D}(t_1)=\left(\frac{i}{\hbar}\right)\langle[\Lambda(t_1),\Theta(t_0)]\rho(t_0)\rangle \tag{2}$$

$$R_{2D}(t_2,t_1)=\left(\frac{i}{\hbar}\right)^2\langle[[\Phi(t_2),\Lambda(t_1)],\Theta(t_0)]\rho(t_0)\rangle \tag{3}$$

$$R_{3D}(t_3,t_2,t_1)=\left(\frac{i}{\hbar}\right)^3\langle[[[\Psi(t_3),\Phi(t_2)],\Lambda(t_1)],\Theta(t_0)]\rho(t_0)\rangle \tag{4}$$

where Ψ, Φ, Λ, and Θ are molecular operators, such as dipole (μ), polarizability (α), first hyperpolarizability (β) *etc.* The initial density operator, denoted as $\rho(t_0)$, is not necessarily the canonical equilibrium density operator, $\rho(-\infty)$. For instance, the IR optical Kerr effect measurement involves a non-equilibrium Raman response function given as $(i/\hbar)\langle[\alpha(t_1),\alpha(t_0)]\rho(t_0)\rangle$, where the initial density operator $\rho(t_0)$ differs from the thermal equilibrium one because of the interaction of vibrational chromophores with intense external IR pulse before the OKE is measured.

By using the vibrational eigenstate representation and taking into account the system–bath interaction, the three response functions defined in eqns. (2)–(4) were obtained as[93,94,132]

$$R_{1D}(t_1)=\left(\frac{i}{\hbar}\right)\theta(t_1)\sum_{ab}P_a(T,t_0)\{\Lambda_{ab}\Theta_{ba}\exp(-i\omega_{ba}t_1)F_{ba}(t_1)-c.c.\} \tag{5}$$

$$R_{2D}(t_2,t_1)=\left(\frac{i}{\hbar}\right)^2\theta(t_2)\theta(t_1)\sum_{abc}P_a(T,t_0)\Big[\Phi_{ab}\Lambda_{bc}\Theta_{ca}\exp(-i\omega_{ba}t_2-i\omega_{ca}t_1)G^{(1)}_{bc}(t_2,t_1)-\Lambda_{ab}\Phi_{bc}\Theta_{ca}\exp(-i\omega_{cb}t_2-i\omega_{ca}t_1)G^{(2)}_{bc}(t_2,t_1)\Big]+c.c. \tag{6}$$

$$R_{3D}(t_3,t_2,t_1)=\left(\frac{i}{\hbar}\right)^3\theta(t_1)\theta(t_2)\theta(t_3)\sum_{\alpha=1}^{4}[H_\alpha(t_3,t_2,t_1)-c.c.], \tag{7}$$

where the auxiliary functions are

$$F_{ba}(t_1)\equiv\exp[-\int_0^{t_1}d\tau_2\int_0^{\tau_2}d\tau_1\xi_{bb}(\tau_2-\tau_1)] \tag{8}$$

$$G^{(1)}_{bc}(t_1,t_2)=\exp\Big\{-\Big[\int_0^{t_2}ds_2\int_0^{s_2}ds_1\xi_{bb}(s_2-s_1)+\int_0^{t_1}ds_2'\int_0^{s_2'}ds_1'\xi_{cc}(s_2'-s_1')+\int_0^{t_2}ds\int_0^{t_1}ds'\xi_{bc}(s+s')\Big]\Big\} \tag{9}$$

$$G^{(2)}_{bc}(t_1,t_2)=\exp\Big\{-\Big[\int_0^{t_2}ds_2\int_0^{s_2}ds_1\xi^*_{bb}(s_2-s_1)+\int_0^{t_1+t_2}ds_2\int_0^{s_2}ds_1\xi_{cc}(s_2-s_1)-\int_0^{t_2}ds_2\int_0^{t_1+t_2}ds_1\xi_{bc}(s_1-s_2)\Big]\Big\} \tag{10}$$

$$\begin{aligned}H_1(t_3,t_2,t_1)=&\sum_{abcd}P_a(T,t_0)\Lambda_{ad}\Phi_{dc}\Psi_{cb}\Theta_{ba}\\&\exp\{i\omega_{cb}t_3+i\omega_{db}t_2-i\omega_{ba}t_1\}\\&\times\exp\Big\{-\int_{t_1}^{t_1+t_2}d\tau_1\int_{t_1}^{\tau_1}d\tau_2\xi^*_{dd}(\tau_1,\tau_2)\\&-\int_{t_1+t_2}^{t_1+t_2+t_3}d\tau_1\int_{t_1+t_2}^{\tau_1}d\tau_2\xi^*_{cc}(\tau_1,\tau_2)\\&-\int_{0}^{t_1+t_2+t_3}d\tau_1\int_{0}^{\tau_1}d\tau_2\xi_{bb}(\tau_1,\tau_2)\\&-\int_{t_1}^{t_1+t_2}d\tau_1\int_{t_1+t_2}^{t_1+t_2+t_3}d\tau_2\xi_{dc}(\tau_1,\tau_2)\\&+\int_{t_1}^{t_1+t_2}d\tau_1\int_{0}^{t_1+t_2+t_3}d\tau_2\xi_{db}(\tau_1,\tau_2)\\&+\int_{t_1+t_2}^{t_1+t_2+t_3}d\tau_1\int_{0}^{t_1+t_2+t_3}d\tau_2\xi_{cb}(\tau_1,\tau_2)\Big\}\end{aligned} \tag{11}$$

$$\begin{aligned}H_2(t_3,t_2,t_1)=&\sum_{abcd}P_a(T,t_0)\Theta_{ad}\Phi_{dc}\Psi_{cb}\Lambda_{ba}\\&\exp\{i\omega_{cb}t_3+i\omega_{db}t_2+i\omega_{da}t_1\}\\&\times\exp\Big\{-\int_{0}^{t_1+t_2}d\tau_1\int_{0}^{\tau_1}d\tau_2\xi^*_{dd}(\tau_1,\tau_2)\\&-\int_{t_1+t_2}^{t_1+t_2+t_3}d\tau_1\int_{t_1+t_2}^{\tau_2}d\tau_2\xi^*_{cc}(\tau_1,\tau_2)\\&-\int_{t_1}^{t_1+t_2+t_3}d\tau_1\int_{t_1}^{\tau_1}d\tau_2\xi_{bb}(\tau_1,\tau_2)\\&-\int_{0}^{t_1+t_2}d\tau_1\int_{t_1+t_2}^{t_1+t_2+t_3}d\tau_2\xi_{dc}(\tau_1,\tau_2)\\&+\int_{0}^{t_1+t_2}d\tau_1\int_{t_1}^{t_1+t_2+t_3}d\tau_2\xi_{db}(\tau_1,\tau_2)\\&+\int_{t_1+t_2}^{t_1+t_2+t_3}d\tau_1\int_{t_1}^{t_1+t_2+t_3}d\tau_2\xi_{cb}(\tau_1,\tau_2)\Big\}\end{aligned} \tag{12}$$

$$
\begin{aligned}
H_3(t_3,t_2,t_1) = \sum_{abcd} & P_a(T,t_0)\Theta_{ad}\Lambda_{dc}\Psi_{cb}\Phi_{ba} \\
& \exp\{i\omega_{cb}t_3 + i\omega_{ca}t_2 + i\omega_{da}t_1\} \\
& \times \exp\Big\{ - \int_0^{t_1} d\tau_1 \int_0^{\tau_1} d\tau_2 \xi^*_{dd}(\tau_1,\tau_2) \\
& - \int_{t_1}^{t_1+t_2+t_3} d\tau_1 \int_{t_1}^{\tau_1} d\tau_2 \xi^*_{cc}(\tau_1,\tau_2) \\
& - \int_{t_1+t_2}^{t_1+t_2+t_3} d\tau_1 \int_{t_1+t_2}^{\tau_1} d\tau_2 \xi_{bb}(\tau_1,\tau_2) \\
& - \int_0^{t_1} d\tau_1 \int_{t_1}^{t_1+t_2+t_3} d\tau_2 \xi_{dc}(\tau_1,\tau_2) \\
& + \int_0^{t_1} d\tau_1 \int_{t_1+t_2}^{t_1+t_2+t_3} d\tau_2 \xi_{db}(\tau_1,\tau_2) \\
& + \int_{t_1}^{t_1+t_2+t_3} d\tau_1 \int_{t_1+t_2}^{t_1+t_2+t_3} d\tau_2 \xi_{cb}(\tau_1,\tau_2) \Big\}
\end{aligned} \tag{13}
$$

$$
\begin{aligned}
H_4(t_3,t_2,t_1) = \sum_{abcd} & P_a(T,t_0)\Psi_{ad}\Phi_{dc}\Lambda_{cb}\Theta_{ba} \\
& \exp\{-i\omega_{da}t_3 - i\omega_{ca}t_2 - i\omega_{ba}t_1\} \\
& \times \exp\Big\{ - \int_{t_1+t_2}^{t_1+t_2+t_3} d\tau_1 \int_{t_1+t_2}^{\tau_1} d\tau_2 \xi_{dd}(\tau_1,\tau_2) \\
& - \int_{t_1}^{t_1+t_2} d\tau_1 \int_{t_1}^{\tau_1} d\tau_2 \xi_{cc}(\tau_1,\tau_2) \\
& - \int_0^{t_1} d\tau_1 \int_0^{\tau_1} d\tau_2 \xi_{bb}(\tau_1,\tau_2) \\
& - \int_{t_1+t_2}^{t_1+t_2+t_3} d\tau_1 \int_{t_1}^{t_1+t_2} d\tau_2 \xi_{dc}(\tau_1,\tau_2) \\
& - \int_{t_1+t_2}^{t_1+t_2+t_3} d\tau_1 \int_0^{t_1} d\tau_2 \xi_{db}(\tau_1,\tau_2) \\
& - \int_{t_1}^{t_1+t_2} d\tau_1 \int_0^{t_1} d\tau_2 \xi_{cb}(\tau_1,\tau_2) \Big\}
\end{aligned} \tag{14}
$$

Here, $P_a(T,t_0)$ is the probability to find the quantum state $|a>$ at time to when the thermal temperature is T. The complex conjugate is denoted as *c.c.* The transition matrix element, for example Θ_{ba}, is defined as $\Theta_{ba} = <b|\Theta|a>$. The entire response functions are determined by the *complex* auto- and cross-correlation functions of the fluctuating transition frequencies defined as

$$\xi_{xy}(\tau_1,\tau_2) \equiv \langle \delta\omega_{xa}(\tau_1)\delta\omega_{ya}(\tau_2)\rangle.$$

By employing a model for the transition frequency fluctuation, such as Markovian (optical Bloch) approximation, Kubo model,[133] or Brownian oscillator model,[134] the response functions can be expressed in terms of the correlation functions of the bath degrees freedom that are coupled to the vibrational or electronic transition between any two quantum states. Depending on the nature of the quantum states involved, one can incoporate the vibrational dephasing or electronic dephasing processes into the formal expressions for the linear and nonlinear response functions.

IV. General advantages of 2D and 3D vibrational spectroscopies in comparison to the 1D vibrational spectroscopy

In Section II, it was shown that various multidimensional vibrational spectroscopies can be devised by properly combining excitation and probing methods. There already exist a number of papers mentioning the general advantages of 2D and 3D vibrational spectroscopies in comparison to the 1D vibrational spectroscopies such as IR, Raman, vibrational circular dichroism, *etc.* Here, we should first define what are multidimensional vibrational spectroscopies that are discussed in this article and what are not. There is so called two-dimensional correlation spectroscopy, where the correlations of IR (or Raman) peaks, when the external macroscopic variables, such as pressure, temperature, concentration *etc.* are modulated, are measured in the two-dimensional frequency space.[135–137] However, these experiments are intrinsically one-dimensional if the experimentally controlled variables are restricted to frequency of the light or time-delay between pulses. Thus, the "multidimensional" means in the present paper that the number of experimentally controlled variables such as frequencies of the external light beams or delay time constants between any two pulses is larger than one.

For example, consider the N-acetyl N′-methyl serine amide that has a number of IR-active vibrational degrees of freedom. If the external IR field frequency is resonant with the amide I vibration, there will appear a peak at $\sim$1650 cm^{-1} in the IR spectrum which is a signature of the existence of the peptide bond in a given molecule.[103] Therefore, the 1D vibrational spectroscopy provides us with information on the distribution of the relatively localized vibrations characterizing each functional group.

In the case of 2D vibrational spectroscopy, due to the doubly-vibrationally-resonant condition, two different IR fields, for example, can be simultaneously resonant with two different vibrational degrees of freedom. Furthermore, in order for the signal not to be zero, the vibrational coupling between two modes (Fig. 5(b), the two modes are amide I vibration and O–H stretching of the serine residue), *via* mechanical or electric anharmonicities, should not vanish. This is only possible when the two vibrational chromophores interact with each other *via* through-bond or through-space connectivity.[73,77,85] This means that the 2D vibrational spectroscopy is a method to measure the spatial proximity of the two vibrational chromophores, *i.e.*, the *two-body interaction*. This is precisely why 2D vibrational spectroscopy can provide much more detailed information on three-dimensional molecular structure.

Much like the 2D vibrational spectroscopy, the 3D vibrational spectroscopy when the three different vibrational degrees of freedom (Fig. 5(c), amide I vibration, OH stretching, and N–H stretching of the second peptide are shown) are simultaneously excited by the three frequency fields can provide through-bond and/or through-space connections among the three modes.[96,132] This is analogous to the measurement of the *three-body interaction*, if each body contains a distinctive vibrational mode.

In the following sections, not only multidimensional vibrational spectroscopies but also other types of ultrafast vibrational spectroscopies will be discussed in more detail.

V. Ultrafast vibrational spectroscopy in centrosymmetric condensed phases

In this section, a few selected ultrafast vibrational spectroscopic methods that has been used to study vibrational dynamics in

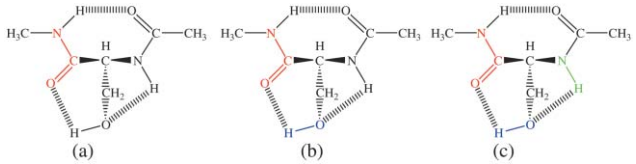

Fig. 5 Non-bonded-interacting N-acetyl N′-methyl serine amide. There are three characteristic intramolecular hydrogen bonding interactions.

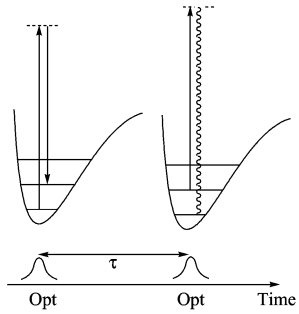

Fig. 6 Pulse configuration and energy level diagram associated with the ultrafast OKE spectroscopy.

isotropic condensed phases will be briefly summarized and discussed.

A. Optical Kerr effect measurement

The most widely used ultrafast vibrational spectroscopic method with femtosecond laser pulses is the optical Kerr effect measurement.[109–120] The excitation-probing process in this case is Epha2–Ppha2 (see Fig. 6), and the associated response function is $R_{1D}(t_1) = (i/\hbar)\langle[\alpha(t_1),\alpha(t_0)]\rho(-\infty)\rangle$.

The first optical pulse of which central frequency is far off-resonant with respect to the electronic transition is used to create a 1D vibrational TG in the sample. Then later, after a finite delay time, τ, the second optical pulse is injected to stimulate the Raman scattering process. Depending on the detection method, either the homodyned or heterodyned signals are measured. Since the excitation and probing steps both are stimulated Raman scattering processes, the Raman-active vibrational degrees of freedom can be studied by using this method. Over the last decade, the OKE measurement has been shown to be an exceptionally useful technique for the investigation of the intermolecular vibrational dynamics in liquids and solutions. Noting that the typical tens of femtosecond pulse has a spectral width of a few hundred wavenumbers, this method is particularly suited to excite and probe the low-frequency liquid vibrational motions. A number of interesting works and suggestions that the measured OKE spectral density can be related to the solvation dynamics and chemical reaction dynamics were studied in detail and the readers should refer to the relevant references.[118,138–142]

B. Ultrafast IR-Raman

The ultrafast IR-Raman method[3,48] is associated with the following sequence of excitation-probing methods, Epop1–Ppop2, and the corresponding response function is the non-equilibrium Raman response function, $R_{1D}(t_1,0) = (i/\hbar)\langle[\alpha(t_1),\alpha(t_0)]\rho(t_0)\rangle$. Note that the initial density matrix, $\rho(t_0)$, is determined by the intense IR-field-matter interaction-induced change of the population, which occurs prior to the incoherent Raman scattering process. The first step in this case involves two IR-field-matter interactions creating a population state on a specific vibrationally excited state. After a finite delay time τ, an optical pulse is injected and then the incoherent Raman scattering spectrum is measured as a function of τ.

As pictorially shown in Fig. 7, the intensity of a specific peak in the incoherent Raman snapshot spectrum at a certain time τ is proportional to the population of the corresponding vibrational state. Therefore, the ultrafast IR-Raman spectroscopy is a useful tool to investigate the intra- and intermolecular vibrational energy redistribution process in time. The IR-Raman method, which was originally discussed by Kaiser and Laubereau, has been extensively used by Dlott and coworkers and they showed that the population relaxation

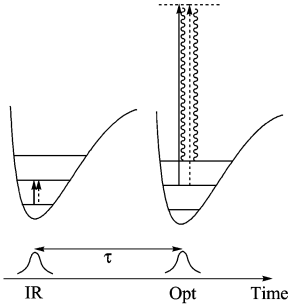

Fig. 7 Pulse configuration and energy level diagram associated with ultrafast IR-Raman spectroscopy. The first IR-pulse generates population state and then the incoherent Raman scattering spectrum is recorded as a function of the delay time τ.

pathways of acetonitrile and other molecular systems can be studied in detail.[44–48]

C. IR pump–probe

Another conceptually simple experiment that is suitable for the investigation of the vibrational energy relaxation is the IR pump–probe, Epop1–Ppop1. The associated response function is $R_{3D}(t_3,t_2,t_1)$ in eqn. (4) with $\psi = \mu$, $\Lambda = \mu$, $\Phi = \mu$, $\Theta = \mu$, and $\rho(t_0) = \rho(-\infty)$. The corresponding pulse configuration and energy level diagram are drawn in Fig. 8.

Although in Fig. 8, only the transient absorption of the weak IR probe beam is shown in the energy level diagram, photobleaching also contributes to the measured IR pump–probe signal. Despite this there are a number of cases where the IR pump–probe method was found to be useful, and the recent experiment using IR pump–probe method to study hydrogen-bonding dynamics in liquids is particularly notable.[143–145] Also, the IR pump–probe method has been effectively used to carry out a structural analysis of the short polypeptides.[33,34,92,146,147] Using an ultrashort (subpicosecond) IR pump pulse, one can create vibrational population and coherence states of the amide I vibrational excitons of polypeptide.[103,104,148] Then, measuring the self-heterodyned IR pump–probe signal and dispersing the generated pump–probe signal field, Hochstrasser and coworkers and Hamm and coworkers were able to obtain a two-dimensional IR pump–probe spectrum. Since the pump and probe IR pulses are short enough to cover the entire range of amide I vibrational excitonic states, the dispersed signal spectrum is a 2D function with respect to the pump and probe field frequencies. Thus, the vibrational excitonic states that are formed by the dipole–dipole interaction between two peptides in a given polypeptide can be explored by the IR pump–probe method and the two-dimensional display of the pump–probe signal provides much more detailed information on the molecular structure of the protein. In particular, the 2D spectrum of the polypeptide tells us about the vibrational anharmonic shifts. Here, the frequency shifts induced by the vibrational coupling between neighboring peptides provide the key information for the structure determination of polypeptides in solution.

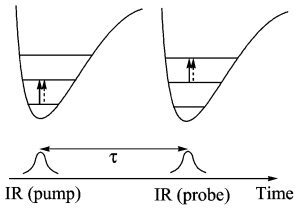

Fig. 8 Pulse configuration and energy level diagram of the IR pump–probe spectroscopy.

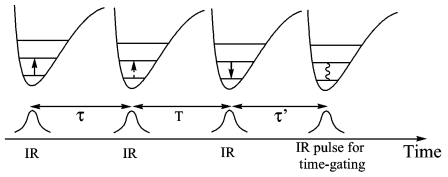

Fig. 9 Pulse configuration and energy level diagram for the four-pulse gated IR photon echo.

D. IR photon echo

The photon echo experiment with electronically resonant pulses has been widely used to study solvation dynamics in condensed phases. The initial goal of the photon echo experiment was to measure the homogeneous broadening in solutions with eliminating the inhomogeneous contribution to the electronic dephasing process.[138,139,149–152] However, it was found out that there is no such truly inhomogeneous (static) broadening in liquids because the time scale of the liquid dynamics and structural changes around a chromophore is very short. In this regard, the photon echo peak shift measurement was found to be extremely useful in studying ultrafast solvation dynamics in solutions.[138,139,153]

Similarly, the IR photon echo with multiple pulses was used to study vibrational dephasing and solvation dynamics of vibrational chromophores in condensed phases.[49–57] The excitation-probing sequence is Epha1–Ephas1–Epha1–Ppha1 (Fig. 9), and the response function is $R_{3D}(t_3,t_2,t_1)$ in eqn. (4) with $\psi = \mu$, $\Lambda = \mu$, $\Phi = \mu$, $\Theta = \mu$, and $\rho(t_0) = \rho(-\infty)$. A number of interesting results were obtained. Particularly, the recent applications of the IR photon echo for the investigation of the protein structure and metal complexes with carbon monoxide ligands were interesting.[57–59,154,155]

As an example, Fayer and coworkers recently applied the IR photon echo method to the composite system consisting of $Rh(CO)_2$acac in dibutyl phthalate.[155] Due to the vibrational coupling between the two CO ligands, there are two types of CO stretching vibrations, *i.e.*, symmetric and antisymmetric modes. By measuring 2D spectra as a function of the first delay time, they were able to show how the 2D IR photon echo method can be used to extract indirect information on the solute–solvent interaction and dynamics.

E. IR-visible four-wave-mixing

IR-visible four-wave-mixing spectroscopy is relatively new and has not been studied much.[73,84,85,89-91,130,131] By combining IR and electronically off-resonant visible fields, a variety of novel four-wave-mixing spectroscopies can be devised. Park and Cho theoretically considered the ultrafast IR–IR–visible sum frequency generation spectroscopy, which is a 2D vibrational spectroscopy.[84] Also other types of IR–Vis four-wave-mixing spectroscopies were theoretically considered.[73,130] The excitation-probing sequence of the IR–IR–Vis sum-frequency-generation spectroscopy is Epha1–Epha1–Ppha2 (Fig. 10), and the response function is $R_{2D}(t_2,t_1)$ in eqn. (3) with $\Lambda = \alpha$, $\Phi = \mu$, $\Theta = \mu$, and $\rho(t_0) = \rho(-\infty)$. The first two IR pulses are used to create two-dimensional vibrational TG and then the stimulated Raman process is used to probe the relaxation of thus created 2D vibrational TG in time domain. Since the first two IR pulses can be short enough to create multiple vibrational coherences, the measured signal can be displayed in 2D frequency space.

The first IR–IR–Vis sum-frequency-generation spectroscopy was used by Bonn *et al.* to study vibrational dynamics and interactions of CO molecules adsorbed on a Ru metal surface.[91] It was shown that intermolecular interactions, mainly the dipole–dipole interaction, between adsorbates can be studied by using the IIV SFG method and the screening effects induced by the lateral interaction between CO molecules could be investigated.

In relation to the IIV SFG in time domain, the frequency-domain IIV difference-frequency-generation experiment was for the first time carried out by Wright and coworkers, so called DOVE IR FWM (doubly vibrationally enhanced IR four-wave-mixing).[89,90,131] For liquid acetonitrile, they were able to observe a cross peak associated with the vibrational coupling between CN and CC stretching vibrations.[89] Since these IR-Vis FWM spectroscopies require double resonances with two-color IR fields, those combination bands, which are so weak that they are hidden under strong fundamental peaks from solvent or other vibrational modes, can be spectrally resolved even for a mixture of acetonitrile and water. This observation suggests that the two-dimensional vibrational spectroscopy involving doubly vibrationally resonant excitations can be used as a useful analytical tool in the future.[90]

F. Six-wave-mixing vibrational spectroscopy

A notable advance in the six-wave-mixing spectroscopy is the recent theoretical and experiment investigations using ultrafast fifth-order 2D Raman scattering spectroscopy.[60–74,80-83,87,88,97–102,128,129] Although Bloembergen and coworkers measured the coherent higher-order Raman emission signal, which is a frequency-domain six-wave-mixing spectroscopy, the theoretical proposal of the fifth-order Raman scattering spectroscopy by Tanimura and Mukamel[60] initiated a number of experimental works since the first attempt by Tominaga and Yoshihara.[63] The fifth-order Raman spectroscopy involves the following sequence of excitation-probing steps, Epha2–Epha2–Ppha2 (Fig. 11), and the associated response function is $R_{2D}(t_2,t_1)$ with $\Lambda = \alpha$, $\Phi = \alpha$, $\Theta = \alpha$, and $\rho(t_0) = \rho(-\infty)$.

The first two vibrational coherence generation steps are achieved by using the two stimulated Raman scattering excitations of vibrational degrees of freedom. Then, thus created 2D vibrational TG is probed by using another stimulated Raman scattering method. Since the total number of field-matter interactions including the final interaction of the matter with the spontaneously fluctuating vacuum field is six, the

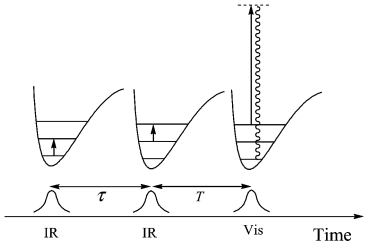

Fig. 10 Pulse configuration and energy level diagram of the IR–IR–Vis sum-frequency-generation spectroscopy. The first two excitation steps are Epha1. The probing method is Ppha2.

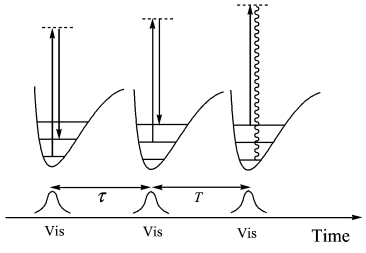

Fig. 11 Energy level diagrams of the fifth-order Raman scattering process. The first two vibrational coherence states are created by the two Epha2 interactions, and followed by the Ppha2 for probing the relaxation of the 2D vibrational transient grating.

fifth-order Raman spectroscopy is a six-wave-mixing spectroscopy. Over the last few years, this experimental method has attracted a lot of attention from experimentalists and theorists, but recently it was found that sometimes the cascading contribution is even dominant over the direct fifth-order Raman process.[80,81,100,129] Blank, Kaufman, and Fleming showed that it is possible to selectively measure the direct fifth-order Raman signal by carefully adjusting the phase matching geometry.[87,88] Combining the 2D Fourier deconvolution theory with experimental data, Kaufman *et al.* were able to extract pure fifth-order Raman response function from the convoluted signal.[83] Nevertheless, the homodyne-detected signal, which is proportional to the square of fifth-order polarization or approximately to the square of fifth-order Raman response function, is not sensitive to the sign change of the corresponding response function. Kaufman *et al.*[88(*b*)] recently reported that the actively phase-locked heterodyne-detected fifth-order Raman signal was for the first time measured and it was found that the signal is in quantitatively good agreement with the response function obtained by the full molecular dynamics simulation carried out by Saito and Ohmine.[97(*b*)] The fifth-order Raman spectroscopy has been mainly used to study vibrational couplings among different liquid intermolecular vibrational degrees of freedom. Since the tens of femtosecond optical pulse has a width of a few hundred wave number in the frequency domain, these pulses cannot be used to excite high-frequency vibrational modes of which frequency is larger than 1000 wave number. However, if the pulse width is as short as a few femtosecond, and also if there is a reliable method to get rid of cascading contribution to the fifth-order Raman signal, the fifth-order 2D Raman spectroscopy will provide extremely useful information on the vibrational coupling between intramolecular modes, between intermolecular vibrational modes, and between intramolecular and intermolecular modes.

Another example of ultrafast vibrational six-wave-mixing spectroscopy is coherent hyper-Raman scattering spectroscopy.[156] In this case, the vibrational excitation-probing sequence is Epha3–Ppha3. The associated response function is that of the hyperpolarizability of the molecular system, *i.e.*, $(i/h)\langle[\beta(t_1),\beta(t_0)]\rho(-\infty)\rangle$. Since the vibrational selection rule offers for hyper-Raman and Raman transitions, one can extract different information on the liquid vibrational dynamics, in comparison to other coherent Raman scattering method such as the optical Kerr effect measurement.

G. Eight-wave-mixing vibrational spectroscopy

Although the fifth-order Raman scattering process in time-domain was first studied in mid 1990's, eight-wave-mixing vibrational spectroscopy, the so called Raman echo spectroscopy, which was theoretically proposed by Loring and Mukamel,[157] was experimentally performed in early 1990's.[158-162] The Raman echo process involves three Epha2's as can be seen in Fig. 12.

The first two field-matter interactions (Epha2) create a vibrational coherence state. Then, the next two field-matter interaction (Epha2), in the particular energy level diagram in Fig. 12, create a population state on the vibrationally excited state. A second vibrational coherence state is generated by the third Epha2 process. Finally, the stimulated Raman scattering field produced by the seventh-order polarization is detected. Since during the final time period vibrational rephasing can occur, this seventh-order nonlinear spectroscopy was called the Raman echo. Although the Raman echo experiment was shown to be successful in elucidating vibrational dephasing processes in condensed phases, the IR photon echo method, which is a four-wave-mixing spectroscopy, has been found to be more practically convenient in comparison to the measurement of an eight-wave-mixing signal. Furthermore, it is not yet clear how one can always effectively remove the undesired cascading contributions to the seventh-order signal.[129]

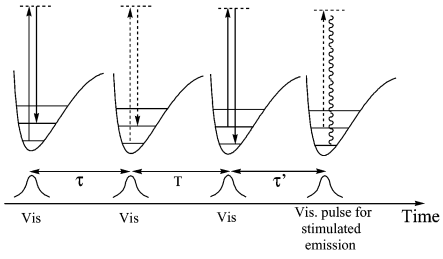

Fig. 12 Raman echo pulse configuration and energy level diagrams.

VI. Ultrafast surface multi-dimensional vibrational spectroscopy in non-centrosymmetric systems on surfaces or at interfaces

In the previous section, a variety of ultrafast vibrational spectroscopies that have been applied to centrosymmetric systems such as liquids, solutions, and glasses were discussed. In the present section, various ultrafast vibrational spectroscopies applicable to non-centrosymmetric molecular systems on surfaces or at interfaces are briefly summarized.

A IR-Vis three-wave-mixing

The most widely used ultrafast vibrational spectroscopy on surfaces and at interfaces is sum-frequency-generation spectroscopy using IR and visible pulses. This method, called IR-Vis Sum-Frequency-Generation (IV-SFG) was pioneered by Shen and coworkers and involves a vibrational excitation with an IR beam which is then followed by the visible pulse initiating a stimulated Raman scattering process.[163–186] Thus, the excitation-probing process is Epha1–Ppha2. Although the conventional IR absorption method has been widely used to study surface vibrational dynamics for a long time, the IV-SFG method has a unique advantage. Since IV-SFG is a second-order nonlinear optical process, it is highly sensitive to the molecular response from those systems lacking centrosymmetry, such as adsorbed molecules on surfaces. Therefore, it is an ideal vibrational spectroscopic tool for the investigation of the vibrational dynamics and chemical reactions on metal surfaces as well as at the gas–liquid, liquid–liquid, and liquid–solid interfaces.

One can use the IV-SFG as a detection method to probe the population relaxation of the vibrationally excited state. Once a non-equilibrium population state is created by the interaction of the vibrational chromophore with an intense IR pulse, the vibrational energy relaxation of the adsorbed molecules can be probed by measuring the intensity of the IV-SFG field.

B. IR-Vis four-wave-mixing

Recently, the IR–IR–Vis sum-frequency-generation process has been experimentally observed by Bonn *et al.*[91] Although they used a single IR pulse, the third-order nonlinear polarization with frequency equal to the sum of the IR–IR–Vis field frequencies was detected. Thus, this is the very first experimental demonstration of surface 2D vibrational spectroscopy. It was found that this novel method can be of use in the investigation of the screening effects on the third-order nonlinear optical process so that the intermolecular interaction between adsorbed molecules can be further studied by using this method.[187] It is desirable to carry out a two-color IIV-SFG experiment[85] for composite molecular systems with two or more different chemical species on surfaces to investigate the vibrational coupling between the two different molecules.

C. Surface IR photon echo

Much like the IR photon echo experiment used to investigate vibrational dephasing processes in condensed phases, the same experimental method has been used to study vibrational relaxation of a chromophore on solid surface.[188] Since the IR photon echo is a useful method to study pure dephasing process without contamination from the static inhomogeneous broadening, the IR photon echo signal provides information on how the adsorbed molecules loses their vibrational coherence memory due to the chromophore–bath interaction.

VII. A variety of theoretically proposed experiments that have not been carried out yet: perspectives I

In the previous sections V and VI, the ultrafast vibrational spectroscopies that have been used to study vibrational dynamics and couplings were briefly summarized. In the present section, novel ultrafast vibrational spectroscopic methods that have not been realized experimentally will be discussed with an emphasis on their differences from other methods outlined in sections V and VI.

A. IR-Visible three-wave-mixing with circularly polarized lights

As mentioned in Section VI-A, the IV-SFG method is found to be of critical use in the surface science. Recently, Shen and coworkers showed that the IV-SFG method can provide quantitative information on the molecular chirality even for isotropic liquids.[189] The origin of the non-zero IV-SFG signal from liquids is from the non-zero antisymmetric polarizability tensor elements of *chiral* molecules, due to the breakdown of the Born–Oppenheimer approximation.[190] However, their experiment is in the frequency-domain so that the evolution of the chiral molecules in solutions, such as protein folding, cannot be investigated by using their experimental configuration. The author recently studied a novel nonlinear optical process that can be effectively used to time-resolve vibrational optical activity of chiral molecules in solution.[108] This circularly polarized (CP) IV-SFG requires a circularly polarized IR beam to create a vibrational coherence state, and then a delayed electronically off-resonant visible pulse is used to probe the vibrational TG. Therefore, the excitation-probing process is Epha4–Ppha2, and the associated energy level diagram is shown in Fig. 13.

Within the electric dipole approximation, the second-order (three-wave-mixing) process in isotropic molecular system such as liquids and solutions vanishes due to the orientational averaging over the random distribution of molecular orientations. However, because of the breakdown of the Born–Oppenheimer approximation and the presence of the electric quadrupole-field interaction, the CP IV-SFG signal does not vanish when the molecule is chiral. By using particularly chosen detection schemes as discussed in ref. 108, one can selectively measure the *anti*-symmetric part of the molecular polarizability and the electric-quadrupole-field interaction-induced contribution to the CP IV-SFG signal separately. Therefore, it was suggested that the CP IV-SFG method can be of critical use in studying the protein folding process, if the folding or unfolding of a given protein is initially triggered by other methods such as an intense IR field induced temperature jump method.[191]

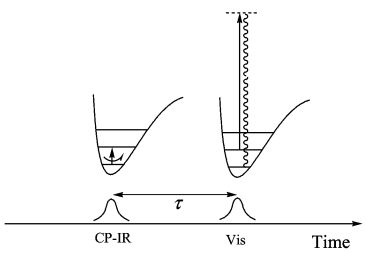

Fig. 13 Pulse configuration and energy level diagram of the CP IV-SFG process. Note that the IR field is circularly polarized.

B. IR-OKE

The ultrafast IR-Raman method, as discussed in Section V-B, has been used to study vibrational energy relaxation of a vibrationally excited state pumped up by an interaction of the vibrational chromophore with an intense IR pulse. There, the probing method is Ppop2, that is to say, the incoherent Raman scattering signal is detected. Due to the incoherent nature of the probing step, it has a distinctive advantage. The measured Raman spectrum contains critical information on the time-dependent populations of *all* Raman-active vibrational modes simultaneously. That is to say, the time-dependent Raman spectra correspond to the snapshot spectra of the population distribution at a given time. Although the ultrafast IR-Raman method has this advantage over the other coherent method, the detection sensitivity is quite low because the incoherently emitted light has to be detected. The author theoretically studied so called IR-OKE method (see Fig. 14 for the pulse configuration and energy level diagrams).[121]

The excitation step is to create a population state, $|1,0><1,0|$, on the vibrational excited state. Then, after the first delay time τ, the optical Kerr effect measurement is performed. During $_{\tau}$, the system evolves a vibrational energy redistribution over the other intra- and intermolecular vibrational degrees of freedom. Therefore, the measured OKE signal in time or its Fourier transformed spectrum will be a function of the first delay time τ, and the time-dependent OKE signal or OKE spectra will give us information on the vibrational energy redistribution. Since the OKE measurement has been found to be exceptionally useful for the investigation of the liquid vibrational dynamics over the last decade, the IR-OKE method will be of critical use to elucidate the vibrational energy transfer from a target vibrational chromophore to the solvent bath degrees of freedom (Fig. 15).

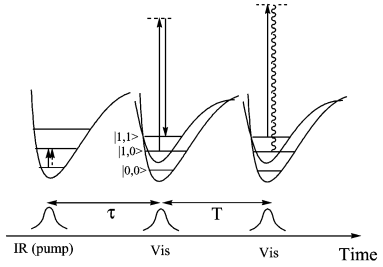

Fig. 14 Pulse configuration and energy level diagram for the IR-OKE method. For instance, if the coupled modes are bath degrees of freedom, the vibrational energy dissipation of the solute vibration to the bath modes can be studied by using IR-OKE method.

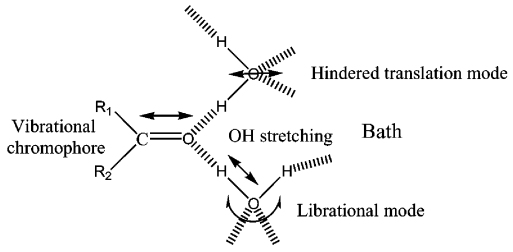

Fig. 15 A schematic picture of vibrational interaction between the IR-pumped vibrational degree of freedom and the solvent vibrational modes. Hindered translation and rotation (librational) motions, and OH stretching motion of solvent molecules are pictorially shown in this figure.

C. Vibrational/electronic FWM

The ultrafast vibrational spectroscopies considered so far focused on the vibrational dynamics and coupling on the potential energy surface of the electronic ground state. On the other hand, the *electronic* photon echo spectroscopy, such as photon echo peak shift measurement, has been found to be useful in studying solvation dynamics in solutions.[138,139,153] In this case, the chromophore-solvent dynamics, which modulates the *electronic* transition frequency, can be indirectly measured by using the electronic photon echo methods. However, there is no experimental method to directly measure the vibrational/electronic couplings induced by the chromophore–solvent interaction. Recently, a couple of nonlinear optical spectroscopies particularly designed to investigate the correlation between vibronic coupling and vibrational coupling has been proposed.[192] The key idea is that both the vibrational coherence state and electronic coherence state are generated in a given nonlinear optical process, as can be seen Fig. 16.

The first method (the left panel of Fig. 16) involves an off-resonant stimulated Raman scattering and a resonant Raman scattering, Epha2–(resonant)Ppha2. The corresponding response function in this case is $R_{2D}(t_2,t_1) = (i/\hbar)^2\langle[[\mu(t_2),\mu(t_1)],\alpha(t_0)]\rho(-\infty)\rangle$. The Epha2 excitation process will create a 1D vibrational TG on the ground potential energy surface, and then the electronically resonant pulse is used to probe the vibrational and vibronic couplings as a function of the delay time T. The second method, depicted in the right panel of Fig. 16, involves Epha1–(resonant)Ppha3, and the response function in this case is $R_{2D}(t_2,t_1) = (i/\hbar)^2\langle[[\mu(t_2),\alpha(t_1)],\mu(t_0)]\rho(-\infty)\rangle$. The excitation step is just a creation of the vibrational coherence state by an IR pulse. After a finite delay time T, a two-photon resonant optical pulse is used to probe the vibrational/electronic coupling induced by the chromophore–solvent interaction. This method will provide unique information on the correlation between the vibrational coupling and vibronic coupling of chromophores in condensed phases. As emphasized in ref. 192, the ultrafast OKE method is useful to study intermolecular vibrational dynamics in liquids, but is limited to Raman-active modes. On the other hand, far-IR spectroscopy can be used to study IR-active low-frequency intermolecular vibrational motions in liquids. Now, the same types of intermolecular vibrational modes are involved in the vibronic coupling when the chromophore undergoes an electronic transition. However, there is no experimental method distinguishing which intermolecular liquid vibrations, either IR-active or Raman-active, are strongly coupled to the electronic transition. In this regard, the vibrational/electronic FWM spectroscopies proposed in ref. 192 should be of use in the investigation of the coupling strength of the intermolecular liquid vibrations when the chromophore is electronically excited. This will also be useful in studying protein structure analysis. The protein vibrational degrees of freedom are likely to be strongly coupled to the electronic transition of the peptide bonds. If the coupling pattern is sensitive to the three-dimensional structure of the peptide backbones, the resultant vibrational/electronic FWM spectrum will provide some information on the peptide conformation.

D. IR–IR–Vis SFG or DFG

The first experimental demonstration of the IR–IR–Vis SFG method was performed by Bonn *et al.*,[91] the molecular system under investigation was CO molecules on Ru metal surface. Since the vibrational chromophores are all identical, *i.e.*, C–O stretching motions, the 2D characteristic feature of the IIV-SFG spectroscopy was not fully explored yet. Suppose that a mixture of different molecules are adsorbed on a metal surface and in particular two vibrational chromophores have different frequencies, ω_1 and ω_2. If the two IR field frequencies, ω_{IR1} and ω_{IR2}, are tuned to be resonant with these two vibrational frequencies, *i.e.*, $\omega_{IR1} = \omega_1$ and $\omega_{IR2} = \omega_2$, the IIV-SFG process becomes enhanced by the doubly resonant vibrational excitations. Then, the cross peak at ($\omega_{IR1} = \omega_1$, $\omega_{IR2} = \omega_2$) is a characteristic one carrying quantitative information on the vibrational coupling between the two vibrational chromophores. This combination band can be studied by using conventional IR spectroscopy. However, if this combination band is weak and hidden under strong fundamental bands, the 2D IIV-SFG measurement will be an alternative way of studying the vibrational-interaction-induced combination band. Since the vibrational interaction is a function of intermolecular distance between the two chromophores,[77,85] the intensity of the cross peak is likely to be very sensitive to the average intermolecular distance between the two different chromophores. It is this distance-dependence of the 2D vibrational cross peak that the 2D vibrational spectroscopy can be considered to be a promising tool for the investigation of the vibrational coupling between two local vibrational degrees of freedom and consequently of the structure determination of complex molecular system. Although the above discussion focused on the adsorbed molecules on metal surfaces. The same argument can be given for the complicated polyatomic molecules. As pictorially discussed in ref. 73, any two localized vibrational modes, such as amide I vibration and other peptide vibration, will produce a corresponding cross peak in the 2D IIV-SFG or IIV-DFG (IIV difference-frequency-generation) spectrum, as long as the two localized modes are spatially close to each other so that the vibrational interaction can induce mechanical and electric anharmonic couplings.

E. IR–Vis–IR FWM

In the case of IIV-SFG or DFG, the detected signal field is in the range of optical field frequency since the probing step involves a stimulated Raman scattering, *i.e.*, Ppha2. However, as theoretically proposed in ref. 73 and 76, one can use the

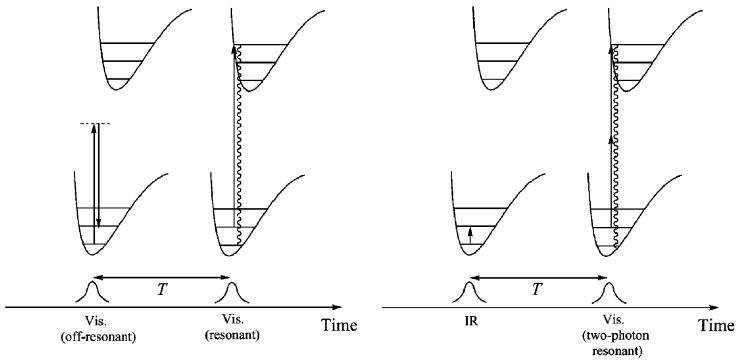

Fig. 16 Two vibrational/electronic FWM schemes.

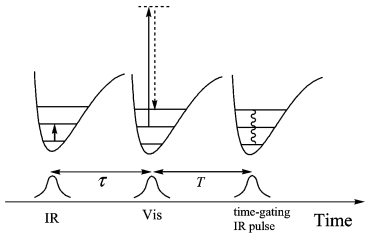

Fig. 17 Pulse configuration and energy level diagram of the IR-Vis-IR FWM spectroscopy. One can use the second IR pulse for the time-gating.

following excitation-probing scheme, Epha1–Epha2–Ppha1 with the associated response function, $(i/h)^2\langle[[\mu(t_2),\alpha(t_1)],\mu(t_0)]\rho(-\infty)\rangle$. The first vibrational coherence state generation is achieved by using an IR pulse. The second vibrational coherence state is created by the electronically off-resonant visible pulse *via* a stimulated Raman process. Then, the relaxation of thus created 2D vibrational TG is probed by detecting the emitted IR field intensity, *i.e.*, Ppha1 method (Fig. 17).

Although this method is slightly different from the IIV-SFG or DFG, the first two vibrational excitations require the involved vibrational modes to be both IR- and Raman-active. On the other hand, IIV-SFG requires the vibrational mode to be IR-active, whereas the fifth-order 2D Raman spectroscopy is useful to study Raman-active modes. Thus, the IR-Vis-IR FWM spectroscopy outlined above will provide a complementary information on the 2D vibrational dynamics and coupling.

F. Surface 2D vibrational spectroscopy

Ultrafast vibrational spectroscopy for molecules on surfaces or at interfaces was briefly mentioned in Section VI, for example the IV-SFG and IR photon echo methods. However, there does not exist any experimental attempt to apply the 2D vibrational spectroscopies recently suggested in ref. 78. Although the IIV-SFG experiment on CO molecules on Ru metal surface was achieved recently,[91] the IIV-SFG method is a four-wave-mixing process so that, unlike the second-harmonic or sum-frequency-generation spectroscopies, it is not surface-specific. Thus, a variety of second-, fourth-, and sixth-order nonlinear optical spectroscopies were theoretically proposed recently. The pulse configurations and energy level diagrams of three representative methods are shown in Fig. 18.

The first scheme, Fig. 18(a), is nothing but an IR sum-frequency-generation so that there is no need to describe it further. The second and third schemes, Fig. 18(b) and (c), are fourth-order nonlinear optical processes, and they differ from each other by the excitation-probing methods. The second one involves Epha1–Epha2–Ppha2 with the response function, $(i/h)^2\langle[[\alpha(t_2),\alpha(t_1)],\mu(t_0)]\rho(-\infty)\rangle$, whereas the third one involves two Epha1 steps with Epha3 (stimulated hyper-Raman scattering) probing method so that the corresponding response function is $(i/h)^2\langle[[\beta(t_2),\mu(t_1)],\mu(t_0)]\rho(-\infty)\rangle$. Since these three- or five-wave-mixing spectroscopies are even order nonlinear optical processes, the signal becomes nonzero only for those molecular systems with a non-centrosymmetry, such as adsorbed molecules on surfaces of at interfaces. Much like the other types of 2D vibrational spectroscopies developed for the investigation of the vibrational coupling of chromophores in isotropic condensed phases, these *surface* 2D vibrational spectroscopies will be of use in studying interactions between vibrational chromophores on surfaces.

G. 2-Color IR photon echo

The IR photon echo, which is a four-wave-mixing process, has recently been a central tool in the investigation of the structural analysis of peptides. Since it involves two vibrational coherence state evolutions, the analogies between two-pulse IR echo and COSY-NMR and between the three-pulse IR echo with NOESY-NMR were discussed before.[57,62,147] However, due to the limited spectral band width of the subpicosecond IR pulse, only one type of vibrational chromophore could be studied by using the one-color IR photon echo. Hochstrasser and coworkers used the IR photon echo to study the amide I vibrational excitons of polypeptide. Tokmakoff and coworkers and Fayer and coworkers used the time-gated IR photon echo to investigate the vibrational coupling between two carbon monoxide ligands in dicarbonylactylacetonato rhodium(I) compound. In both cases, either amide I vibration or CO vibration was only under investigation. These cases are similar to the situation where one type of proton in a given polyatomic molecule and its splitting due to the *J*-coupling were only observed in the 1D NMR spectrum. Therefore, the full two-dimensional IR photon echo experiment, which measures vibrational coupling between two distinctively different vibrations, such as amide I vibration and amide III vibration for example, has not been performed yet.

In order to achieve this goal, one can use much shorter IR pulses so that the spectral band width of the IR pulse is broad enough to cover a larger range of frequencies. However, even in this case the breakdown of the slowly-varying-amplitude approximation will become a critical issue and it will make difficult to interpret the experimental result. An alternative

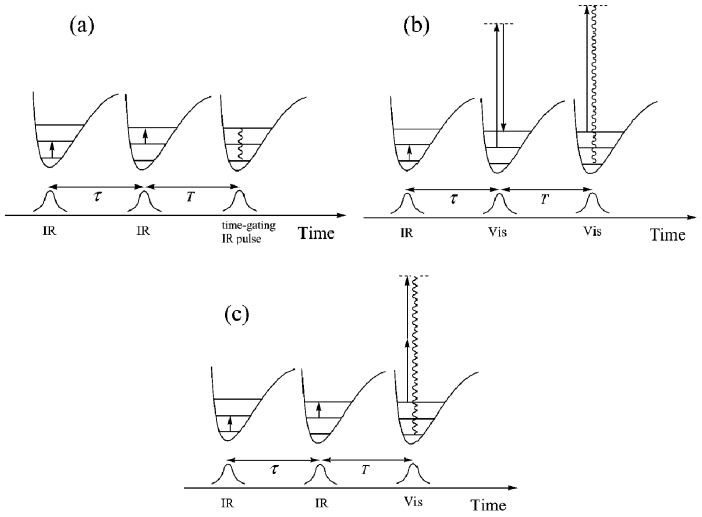

Fig. 18 Schematic diagrams of the three representative surface 2D vibrational spectroscopies.

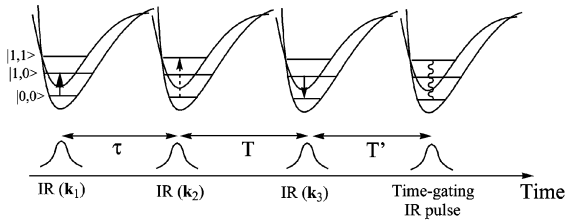

Fig. 19 Energy level diagram and pulse configuration of the 2-color IR photon echo. The wave vectors of each IR fields are shown in the figure and the corresponding frequencies are denoted as ω_j (j = 1,2,3) and $\omega_1 = \omega_3$.

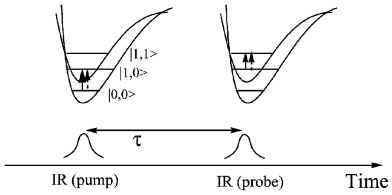

Fig. 20 Two-color IR pump–probe spectroscopy. The field frequencies of the pump and probe pulses are denoted as ω_{pu} and ω_{pr}, respectively.

approach to obtaining the full 2D spectrum with the IR echo technique is to use two-color IR pulses so that the two frequencies are simultaneously resonant with two different vibrational degrees of freedom.[132] As can be seen in Fig. 19, the wave vector of the echo field in this case is $\boldsymbol{k}_3 + \boldsymbol{k}_2 - \boldsymbol{k}_1$. In the specific case shown in Fig. 19, the vibrational chromophore undergoes the following sequence of vibrational transitions, $|0,0><0,0| \rightarrow |1,0><0,0| \rightarrow |1,0><1,1| \rightarrow |0,0><1,1| \rightarrow |0,0><0,0|$. Since it involves two two-quantum transitions, from $<0,0|$ to $<1,1|$ and from $<1,1|$ to $<0,0|$, the mechanical or electric anharmonicities are required to be nonzero. Then, the 2D spectrum with respect to the two field frequencies, ω_1 and ω_2, should contain information on the vibrational coupling between two different modes. Nevertheless, the signal intensity in this case is likely to be much smaller than the one-color IR echo so that one may have to use heterodyne detection method to measure the echo field amplitude.

H. 2-Color IR pump–probe 2D vibrational spectroscopy

The two-color IR pump–probe method, Epop1–Ppop1, has been used to study vibrational energy relaxation processes. However, it has not been used to study vibrational coupling between two different vibrational chromophores. Of course, the vibrational energy relaxation is a phenomenon associated with the mechanical anharmonic couplings between vibrational degrees of freedom. However, the strength of the vibrational coupling cannot be directly extracted from the measured signal only reflecting the population change of the initially pumped excited state. Over the last few years, the one-color IR pump–probe method with proper dispersion detection scheme was found to be a very useful tool in obtaining 2D IR spectra of polypeptides.

In this case, the vibrational-coupling-induced off-diagonal peaks for short polypeptides were observed and the experimental results were used to determine 3D structure of di- or tripeptides in liquids. However, similar to the limitation of the one-color IR photon echo, the one-color IR pump–probe has a limit in the frequency tunability so that the vibrational coupling between two distinctively different vibrational degrees of freedom cannot be studied. Thus, the two-color IR pump–probe spectroscopy ($\omega_{pu} \neq \omega_{pr}$) with measuring dispersed signal spectrum will be a useful method in this regard (Fig. 20).[132] Since the pump–probe spectroscopy is to measure the difference between the probe absorption when the pump pulse was present and that when there was no pump pulse, if the two vibrational degrees of freedom are perfect harmonic oscillators, *i.e.*, there is no vibrational coupling between any two modes, the pump–probe signal becomes zero. This is precisely why the existence of the cross peak in the 2D IR pump–probe spectrum is strong evidence that the two modes are anharmonically coupled to each other.

I. Triply resonant 2D vibrational spectroscopy

A variety of 2D vibrational spectroscopies have used vibrational excitation methods to create 2D vibrational TG in the ground electronic state. Then, the probing involves a vibrational transition *via* IR emission or stimulated Raman (or hyper-Raman) scattering processes. Thus, the visible fields involved in the Ppha2 and Ppha3 are deliberately controlled to be electronically off-resonant. However, as discussed in ref. 193, one can use electronically resonant field to probe the relaxation of the 2D vibrational TG. Since doubly resonant excitations between any two vibrational states and one electronically resonant transition are involved, these spectroscopies are classified as triply resonant 2D vibrational spectroscopy. Although five different experimental schemes were theoretically investigated in ref. 193, two examples are briefly discussed here (Fig. 21).

The first scheme, Fig. 21(a), involves two Epha1 processes with (resonant) Ppha2, whereas the second scheme, Fig. 21(b), involves two Epha2 processes though the probing method is identical to the first one. These two methods differ slightly from the IIV-SFG and fifth-order 2D Raman scattering spectroscopies because of the resonant nature of the probing steps. Since the probing step involves a single electronic transition, not only the 2D vibrational dynamics but also the vibronic coupling can be studied by using this method. The latter aspect is the key difference from the off-resonant analogues. Although

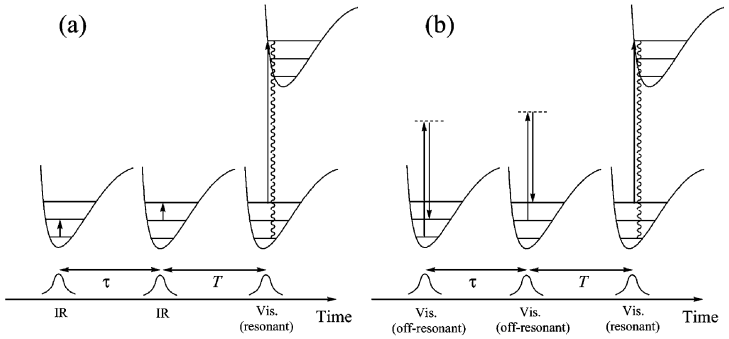

Fig. 21 Energy level diagrams and pulse configuration of the triply resonant 2D vibrational spectroscopy. Note that the two vibrational transition probabilities are enhanced by the double resonances and the electronic transition is resonantly enhanced by the resonant optical pulse.

one can expect an increase of the signal-to-noise ratio due to the electronic resonant enhancement, a laser source that is capable of exciting both vibrational and electronic degrees of freedom is required. Thus, the molecular systems that can be studied by using these methods are likely to be limited.

J. 3D vibrational spectroscopies

The response functions associated with various 3D vibrational spectroscopies were recently studied.[96,132] Here, the three-dimension strictly means that three vibrational coherence states are generated during the nonlinear optical processes. Therefore, other types of correlation effects, such as temperature change, concentration change *etc.*, are not included as an additional dimensionality. As briefly discussed in Section II-D above, the 3D vibrational TG can be created by combining three vibrational excitation methods outlined in Section II, *i.e.*,

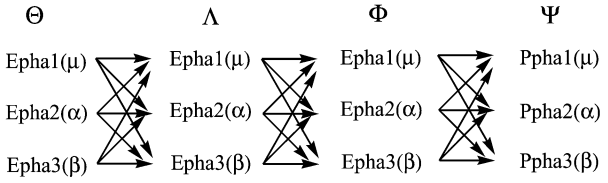

From the above schemes, it is found that there are totally 81 different ways to carry out 3D vibrational spectroscopic measurements. Each of them differ from each other *via* the excitation sequence and probing method. Although some of them are likely to suffer from the notorious cascading contributions, there will be a whole new research area when the full 3D vibrational spectroscopy is experimentally realized. A few suggestions and perspectives were discussed in ref. 96 and[132].

Perhaps, the most simple method is the IR–IR–IR sum- or difference-frequency-generation spectroscopy, when the three IR field frequencies are independently tunable. Since the vibrational transition in this case requires a multi-quantum transition, the signal will be very small indeed and the heterodyne detection technique is likely to be necessary. The clear advantage of the 3D vibrational spectroscopy is that it provides huge number of peaks for a given polyatomic molecules. This means that the 3D vibrational spectrum contains much more detailed information on the 3D structure of the target molecule and provides a 3D vibrational coupling map. Note that the 1D spectrum is a 1D map revealing the presence of each vibrational chromophore. The 2D spectrum is like a 2D map providing information on the vibrational coupling between two modes. Thus, the 3D vibrational spectrum provides far more detailed information on the vibrational coupling among three different modes. This is completely analogous to the 3D NMR spectroscopy in comparison to the 1D or 2D NMR.

K. Comparison between reduced 2D vibrational spectroscopy and genuine 2D vibrational spectroscopy

The IR photon echo and IR pump–probe spectroscopies have been extensively used recently and they were referred to as a 2D IR spectroscopy. However, the associated response functions are 3D vibrational response function defined in eqn. (4). Then, why do these methods belong to 2D spectroscopy and not 3D spectroscopy? It is basically because the number of vibrational coherences involved in these nonlinear optical processes is two instead of three. Thus, these two methods should be called a *reduced* 2D vibrational spectroscopy, in comparison to the *genuine* 2D vibrational spectroscopy. In order to clarify this issue, consider the conventional IR photon echo (Fig. 9). The system evolves two vibrational coherence states during τ and τ', whereas the population period is T. In comparison to the 2-color IR photon echo,[132] which is a true 3D vibrational spectroscopy, the number of vibrational coherence states involved in the IR photon echo method used by Hochstrasser and coworkers and later by others, is two. This is why the IR photon echo was considered to be a 2D vibrational spectroscopy. Similarly, the IR pump–probe spectroscopy also involves two vibrational coherence state evolutions and thus it was classified as a 2D vbrational spectroscopy. However, the associated response functions for these two methods are the vibrational response function given in eqn. (4), not the 2D vibrational response function in eqn. (3).

In contrast, the fifth-order Raman scattering, IR–IR–Vis sum- or difference-frequency-generation spectroscopy, and many others discussed in the present paper are associated with the 2D vibrational response function in eqn. (3) so that we will call these methods a genuine 2D vibrational spectroscopy. Are there any differences between the reduced 2D vibrational spectroscopy and the genuine 2D vbirational spectroscopy? The answer is yes and lies in the difference between the 2D and 3D vibrational response functions. Simply speaking, the number of molecular parameters, such as mechanical anharmonic coefficients and electric anharmonicities of the dipole and polarizability, required in the calculation of the 3D response function is significantly larger than that of the 2D response function. For example, in the weak anharmonicity limit and with factorization approximation, the total number of distinct components contributing to the 2D vibrational response function was found to be three (see refs. 65,[66] and[73]). On the other hand, the number for the 3D vibrational response function is 17.[96] This means that the analysis of the reduced 2D vibrational spectrum, *i.e.*, the ratios of the cross peaks to the diagonal peaks, is likely to be very difficult in comparison to that of the genuine 2D vibrational spectrum. Perhaps, this difficulty may not be a serious obstacle if one is interested in only one type of vibrational motion, as mentioned above. However, as the 2D vibrational spectroscopy develops in the future, the range of accessible frequencies will increase and thus the multiple couplings among many different types of vibrational motions will be observed. Then, how many molecular parameters, such as mechanical and electric anharmonicities, are required for the interpretation of the experimental results, will become a critical issue for determining the utility of the 2D (or even 3D) vibrational spectroscopy in general? The same problem is evident in 3D NMR in comparison to 2D NMR.

VIII. Applications of the ultrafast vibrational spectroscopy in condensed phases: perspectives II

Ultrafast vibrational spectroscopies recently received much attention because they can be used to study a number of different chemical, physical, and even biological processes in real time. As briefly mentioned in the Introduction, most of the previous applications of ultrafast vibrational spectroscopies were to elucidate vibrational dephasing and energy relaxation processes. Certainly, these issues are the most crucial ones in understanding chemical reaction dynamics in condensed phases. However, just recently the ultrafast IR pump–probe and IR photon echo techniques have been found to be useful tools in determining 3D molecular structure of small molecules such as dipeptides dissolved in liquids. This new development seems to be quite promising, particularly when it is noted that the timescale of ultrafast vibrational spectroscopy is of the order of picoseconds —this timescale is indeed ultrafast in comparison to that of typical NMR spectroscopy. The key difference between these recent studies and other more or less conventional studies lies in which molecular properties are experimentally measured. Conventional applications of

time-resolved vibrational spectroscopy focus on the lifetime of a given quantum state or the phase relaxation rate of a single vibrational coherence state. On the other hand, the recent 2D and 3D vibrational spectroscopies in condensed phases are used to measure the vibrational coupling strength *via* peak intensity analysis. The latter information relates to more fundamental properties, whereas the population relaxation is a consequence of the vibrational couplings. In this section, several possible applications and perspectives of the ultrafast multidimensional vibrational spectroscopy will be discussed.

A. Chemical reaction dynamics

The first and most important application of the ultrafast vibrational spectroscopy has to be understanding chemical reaction dynamics in condensed phases including solutions, surfaces, and interfaces. For these applications, one should bear in mind the advantages of multidimensional spectroscopy emphasized in Section IV, in comparison to other 1D vibrational spectroscopies. The spatial connectivity between any two different vibrational degrees of freedom *via* through-bond or through-space interactions is the key information that can be extracted from the time-dependent multidimensional spectra. Thus, in general, by properly choosing the two vibrational degrees of freedom directly reflecting the chemical reaction pathway, one can in principle follow the chemical reaction dynamics in real time. To this end, the timescale of the chemical reaction shouldn't be too fast.

Intramolecular vibrational energy redistribution. The first phenomenon closely related to the chemical reaction dynamics is the intramolecular vibrational energy redistribution process. Although the ultrafast IR-Raman spectroscopy was demonstrated to be a highly useful method for such an investigation, its difficulty in detecting the weak *incoherent* Raman scattering signal is a serious drawback for this method to be widely used to study IVR process of reactive species in condensed phases. Thus, other types of ultrafast multidimensional vibrational spectroscopy, which detect the *coherent* signal, should also be sought in the near future. One candidate would be the 2-color IR pump–probe method. As formulated in ref. 121 (see Appendix C), if the pump and probe field frequencies are independently tunable, it is possible to measure the non-equilibrium IR response function containing information on the state-to-state vibrational population redistribution in time domain. However, this method is also likely to be difficult because one should have IR laser source capable of freely tuning the IR frequency. Once this experimental difficulty is overcome, there are a number of interesting chemical and physical systems that can be investigated by using the 2-color IR pump–probe spectroscopy.

Vibrational dephasing. The second important issue is to understand the vibrational dephasing processes in condensed phases. As discussed before, the 1-color IR photon echo method has been extensively used to study this phenomenon. An alternative method is to use the IR–IR–Vis difference-frequency-generation spectroscopy as shown in ref. 194. Also, as the laser sources and related technology develop, the 2-color IR photon echo or other degenerate 3D vibrational spectroscopic methods will be interesting tools for the investigation of the vibrational relaxation and coupling changes during a given chemical reaction.[132]

Solvent role in a chemical reaction. Since the beginning of the physical chemistry, the role of the solvent molecules in a given chemical reaction has been a central theme in the physical chemistry research. The first theoretical attempt by Kramers has been found to be useful in describing the chemical reaction dynamics in liquids.[195] In 1980's, Kramers's theory was extended by Grote-Hynes and Hanggi by taking into account the memory effect of the surrounding bath degrees of freedom.[196,197] These theories and new developments[17,197,198] have been applied to a number of chemical reactions and found to be extremely useful. However, there is still a lack of way to get direct information on how each individual solvent molecule participates in the chemical reaction. In other words, instead of modeling the solvent role in a chemical reaction by the time-dependent friction kernel, physical chemists might want to see how the solvent nuclear degrees of freedom are excited or de-excited during the process of a chemical reaction, *i.e.*, *molecular description of the fluctuation–dissipation phenomenon*. In this regard, the ultrafast 2D vibrational spectroscopy can be used to achieve this goal. Suppose that there is an indicating vibrational chromophore of the reactive species and which is strongly coupled to a particular solvent vibrational motion. Now, let's denote the associated frequencies are ω_{solute} and ω_{solvent}. If the two controllable frequencies, ω_1 and ω_2, are tuned to be resonant with ω_{solute} and ω_{solvent}, *i.e.*, $\omega_1 \approx \omega_{\text{solute}}$ and $\omega_2 \approx \omega_{\text{solvent}}$. Only when the two characteristic modes are vibrationally coupled to each other does the 2D vibrational spectroscopic signal not vanish. The cross peak at ($\omega_1 \approx \omega_{\text{solute}}$, $\omega_2 \approx \omega_{\text{solvent}}$) is a direct indicator on how the solvent mode is participated in the chemical reaction. Thus, the entire spectrum as a function of scanned ω_2 and time will provide a detailed picture of the solvent role during a given chemical reaction. This idea is perhaps too much simplified, but an attempt along this line would be of high interest and provide new insights on the solvation effects on the chemical reaction dynamics in condensed phases. A few possible chemical reactions are photo-dissociation, photo-induced electron transfer, proton transfer induced by a photo-dissociation *etc.*

B. Solvation structure and dynamics

Solvation dynamics has been extensively studied over the last two decades. In particular, the fluorescence Stokes shift measurement has been most effectively used to study time-dependent solvation dynamics. The other popular method is to use photon echo peak shift (PEPS) measurement as pioneered by Fleming and coworkers.[138] The PEPS was shown to be useful not only to study ultrafast solvation dynamics but also to quantitatively measure the inhomogeneous width.[153] This aspect has been demonstrated for a molecular system in glasses. In order to theoretically describe the solvation dynamics, a number of interesting approaches were proposed and shown to be successful. As far as the long time solvation dynamics is concerned, the dielectric theories of solvation dynamics were found to be quantitatively successful.[199–201] For the ultrafast part of the solvation process, the instantaneous normal mode theory provided an interesting picture,[202–204] because it is based on the microscopic nature of the liquid intermolecular vibrations. Nevertheless, it is still desired to have an experimental method providing direct information on how the surrounding solvent molecules participate in the solvation dynamics and the formation of the local structure around it. In this respect, the IR pump–probe and IR photon echo methods were found to be useful for such a purpose.[143–145,155] However, those works have focused on the vibrational dynamics of the solute only. Therefore, the solute–solvent interaction-induced changes of the vibrational properties of the *solute* (not both solute and solvent) are only observed.

Then, are there any experimental methods that can be used to study solvation dynamics by watching the vibrational dynamics of both solute and solvent? The obvious candidates are the ultrafast 2D vibrational spectroscopies. As emphasized in Section IV, the 2D vibrational spectroscopy can provide direct information on the coupling between two *spatially separated* vibrational modes. Let's assume that each of the two external field frequencies, which are either IR frequency or

stimulated Raman vibrational frequency, is adjusted to be resonant with the two vibrational chromophores, when one of the two belongs to the solute and the other to the solvent (see the discussion in the above subsection). Then, a time-dependent measurement of the cross peak will give us direct information on the solute–solvent interaction, *i.e.*, the microscopic aspect of the solvation dynamics. Currently, this is under investigation in our group, and our preliminary results show that the local structure of the solvent molecules surrounding a given solute strongly affects to the 2D vibrational response function, and consequently the 2D vibrational spectrum.

C. Vibrational interactions between adsorbed molecules: surface science

The vibrational dynamics of adsorbed molecules on surfaces or at interfaces has been studied by using IR reflection method or IV-SFG spectroscopy, and others. However, the previous experimental methods are all one-dimensional so that only one type of vibrational chromophores were under direct investigation at a time. Therefore, 2D or 3D vibrational spectroscopy, as was emphasized in Section IV, specifically designed for molecular systems on surfaces or at interfaces will be of critical use in studying vibrational interactions among different chemical species on surfaces. For instance, the IR–IR SFG method,[78] which is nothing but a sum-frequency-generation spectroscopy, can be used to study a vibrational coupling process between two different adsorbates. Once the experimental sensitivity issue is overcome, the IR–IR SFG or other surface 2D vibrational spectroscopies discussed in Section VII-F will open up a new research area in surface studies.

Furthermore, as the 2D vibrational spectroscopy can be used to study chemical reaction dynamics in isotropic condensed phases, one can use *surface* 2D vibrational spectroscopy for the investigation of inhomogeneous catalysis, surface melting, wetting, and confinement-induced phase transition, *etc.*

D. Biological applications

The most important applications of the ultrafast multidimensional vibrational spectroscopy could be to biological science.

Structure determination of protein. The IR pump–probe and 2D IR photon echo, though those experimental results reported so far are one-color experiment, have been found to be a useful method for establishing the relationship between the 3D structure of protein and measured signals. As discussed in the present paper, other types of genuine 2D vibrational spectroscopies and two-color IR photon-echo or two-color IR pump–probe spectroscopies will serve as critical tools for this purpose. One example would be to focus on vibrational coupling between two different polypeptide vibrations, such as amide I and amide III vibrations, *etc.*

In addition, one can combine vibrational and electronic spectroscopy, such as triply resonant 2D vibrational spectroscopy or vibrational/electronic FWM spectroscopy discussed in Sec.tion VII. The correlation between two modes that are coupled to both vibrational and electronic transitions of the chromophore, such as a peptide bond, is likely to be sensitive to the 3D structure of the polypeptide backbone.

Although in this paper, we have focused on the ultrafast *vibrational* dynamics, there are multidimensional *electronic* spectroscopies too. As an example, the electronically resonant fifth-order Raman spectroscopy[86] and fifth-order three pulse scattering spectroscopy[205] are alternative ways to get information on the 3D structure of proteins. Suppose the two optical field frequencies are simultaneously resonant with two electronic chromophores, such as phenol ring in a Tyr amino acid and peptide bond in a given protein. If the two-color 2D electronic spectroscopy becomes available, the coupling between these two distinctively different electronic transitions can be used to extract information on the 3D structure of polypeptides.

Protein folding dynamics. As emphasized by several researchers in this area, the key advantage of the ultrafast multidimensional vibrational spectroscopy is its experimentally accessible timescale. Although the protein folding occurs in a wide range of time scales, from picoseconds to seconds, solution NMR cannot be used to study the early part of the protein folding process due to its limited time resolution. In this respect, the ultrafast multidimensional vibrational spectroscopy utilizing IR or visible pulses has a clear advantage over the other techniques. In addition to a number of 2D and 3D vibrational spectroscopies, the CP-IV-SFG (circularly polarized IR-Vis sum-frequency-generation) spectroscopy proposed recently can also be used to study protein folding dynamics since the vibrational optical activity is strongly related to the 3D structure of the protein.

Enzyme catalysis and protein–ligand binding process. Another interesting application of the ultrafast multidimensional vibrational spectroscopy is to investigate the substrate–enzyme interaction. In order for a given enzyme to catalyze a biochemical reaction, the substrate (or ligand) should form a complex in a catalytic site of the enzyme. Tuning the two external field frequencies are resonant with the characteristic vibrational modes of the substrate and enzyme, one can directly measure the formation of the ES complex. Similarly, protein–DNA (or protein–RNA) complexes, antibody–antigen complexes, *etc.* can be other interesting targets to be investigated with ultrafast multidimensional spectroscopy.

IX. Summary

In this paper, a number of ultrafast vibrational spectroscopies in condensed phases including isotropic solutions and molecular systems on surface or at interfaces were discussed. Some of them have already been demonstrated to be useful in studying vibrational relaxation and couplings. Also, a variety of novel ultrafast vibrational spectroscopies were introduced and their specific advantages and disadvantages were mentioned. Although a number of interesting perspectives were presented and discussed in the present paper, there will be lots of experimental difficulties. For example, the most difficult obstacle that one has to deal with in the future is the sensitivity of the multidimensional vibrational spectroscopy. The practical reason why the one-color IR photon echo was only experimentally performed is because the signal intensity is strong enough to detect it. In contrast, the two-color IR photon echo process will become formidably difficult because the involved vibrational transitions are two-quantum process so that the total transition probability, or the signal, is likely to be very small. Once stable and tunable laser sources generating ultra-short IR and visible pulses are available, the ultrafast multidimensional vibrational spectroscopies discussed in this paper will be the central tools for elucidating a wide of range of chemical and biological phenomena.

Acknowledgement

This work was supported by KISTEP *via* Creative Research Initiatives Program (MOST, Korea). The author thanks Professor G. R. Fleming for carefully reading the manuscript, critical comments, and helpful suggestions.

References

1 *Ultrafast Infrared and Raman Spectroscopy*, ed. M. D. Fayer, Marcel Dekker, New York, 2001.
2 *Chem. Phys.*, 2001, **266**, 2/3, 135–365 .

3 A. Laubereau and W. Kaiser, *Rev. Mod. Phys.*, 1978, **50**, 607.
4 K. Wynne and R. M. Hochstrasser, *Chem. Phys.*, 1995, **193**, 211.
5 S. Mukamel, A. Piryatinski and V. Chernyak, *Acc. Chem. Res.*, 1999, **32**, 145.
6 H. Graener and A. Laubereau, *Appl. Phys. B*, 1982, **29**, 213.
7 W. Zinth, C. Kolmeder, B. Benna, A. Irgens-Defregger, S. F. Fischer and W. Kaiser, *J. Chem. Phys.*, 1983, **78**, 3916.
8 J. R. Ambroseo and R. M. Hochstrasser, *J. Chem. Phys.*, 1988, **89**, 5956.
9 N. H. Gottfried and W. Kaiser, *Chem. Phys. Lett.*, 1983, **101**, 331.
10 A. Tokmakoff, B. Sauter, A. S. Kwok and M. D. Fayer, *Chem. Phys. Lett.*, 1994, **221**, 412.
11 X. Hong, S. Chen and D. D. Dlott, *J. Phys. Chem.*, 1995, **99**, 9102.
12 S. Chen, X. Hong, J. R. Hill and D. D. Dlott, *J. Phys. Chem.*, 1995, **99**, 4525.
13 M. Hofmann and H. Graener, *Chem. Phys.*, 1996, **206**, 129.
14 M. Hofmann, R. Zürl and H. Graener, *J. Chem. Phys.*, 1996, **105**, 6141.
15 H. Graener, R. Zürl and M. Hofmann, *J. Phys. Chem.*, 1997, **101**, 1745.
16 J. C. Deàk, L. K. Iwaki and D. D. Dlott, *J. Phys. Chem. A*, 1998, **102**, 8193.
17 G. A. Voth and R. M. Hochstrasser, *J. Phys. Chem.*, 1996, **100**, 13034.
18 D. W. Oxtoby, *Annu. Rev. Phys. Chem.*, 1981, **32**, 77.
19 J. Chesnoy and G. M. Gale, *Adv. Chem. Phys.*, 1988, **70**, 297.
20 J. Owrutsky, D. Raftery and R. M. Hochstrasser, *Annu. Rev. Phys. Chem.*, 1994, **45**, 519.
21 E. J. Heilweil, M. P. Cassassa, R. R. Cavanagh and J. C. Stephenson, *J. Chem. Phys.*, 1986, **85**, 5003.
22 H. Graener, R. Dohlus and A. Laubereau, *Chem. Phys. Lett.*, 1987, **140**, 306.
23 H. Graener, T. Q. Ye and A. Laubereau, *J. Chem. Phys.*, 1989, **90**, 3413.
24 J. D. Beckerle, R. R. Cavanagh, M. P. Cassassa, E. J. Heilweil and J. C. Stephenson, *J. Chem. Phys.*, 1991, **95**, 5403.
25 H. Graener and G. Seifert, *J. Chem. Phys.*, 1993, **98**, 36.
26 H. Graener, G. Seifert and A. Laubereau, *Chem. Phys.*, 1993, **175**, 193.
27 H. J. Bakker, *J. Chem. Phys.*, 1993, **98**, 8496.
28 J. D. Beckerle, M. P. Cassassa, R. R. Cavanagh, E. J. Heilweil and J. C. Stephenson, *Chem. Phys.*, 1992, **160**, 487.
29 A. Tokmakoff, B. Sauter and M. D. Fayer, *J. Chem. Phys.*, 1994, **100**, 9035.
30 A. Tokmakoff, R. S. Urdahl, D. Zimdars, R. S. Francis, A. S. Kwok and M. D. Fayer, *J. Chem. Phys.*, 1995, **102**, 3919.
31 S. Woutersen, U. Emmerichs and H. J. Bakker, *J. Chem. Phys.*, 1997, **107**, 1483.
32 J. Childs and J. D. Beckerle, *J. Chem. Phys.*, 1997, **107**, 319.
33 M. Lim, P. Hamm and R. M. Hochstrasser, *Proc. Natl. Acad. Sci. U. S. A*, 1998, **95**, 15315; P. Hamm, M. Lim and R. M. Hochstrasser, *Phys. Rev. Lett.*, 1998, **81**, 5326.
34 P. Hamm, M. Lim, W. F. DeGrado and R. M. Hochstrasser, *J. Phys. Chem. A*, 1999, **103**, 10049.
35 H. Graener and A. Laubereau, *Appl. Phys. B*, 1982, **29**, 213.
36 W. Zinth, C. Kolmeder, B. Benna, A. Irgens-Defregger, S. F. Fischer and W. Kaiser, *J. Chem. Phys.*, 1983, **78**, 3916.
37 J. R. Ambroseo and R. M. Hochstrasser, *J. Chem. Phys.*, 1988, **89**, 5956.
38 N. H. Gottfried and W. Kaiser, *Chem. Phys. Lett.*, 1983, **101**, 331.
39 A. Tokmakoff, B. Sauter, A. S. Kwok and M. D. Fayer, *Chem. Phys. Lett.*, 1994, **221**, 412.
40 X. Hong, S. Chen and D. D. Dlott, *J. Phys. Chem.*, 1995, **99**, 9102.
41 M. Hofmann and H. Graener, *Chem. Phys.*, 1996, **206**, 129.
42 M. Hofmann, R. Zürl and H. Graener, *J. Chem. Phys.*, 1996, **105**, 6141.
43 H. Graener, R. Zürl and M. Hofmann, *J. Phys. Chem.*, 1997, **101**, 1745.
44 J. C. Deàk, L. K. Iwaki and D. D. Dlott, *Opt. Lett.*, 1997, **22**, 1796.
45 S. Chen, X. Hong, J. R. Hill and D. D. Dlott, *J. Phys. Chem.*, 1995, **99**, 4525.
46 J. C. Deàk, L. K. Iwaki and D. D. Dlott, *J. Phys. Chem. A*, 1998, **102**, 8193.
47 L. K. Iwaki and D. D. Dlott, *Chem. Phys. Lett.*, 2000, **321**, 419.
48 D. D. Dlott, *Chem. Phys.*, 2001, **266**, 149.
49 D. Zimdars, A. Tokmakoff, S. Chen, S. R. Greafield and M. D. Fayer, *Phys. Rev. Lett.*, 1993, **70**, 2718.
50 A. Tokmakoff and M. D. Fayer, *J. Chem. Phys.*, 1995, **103**, 2810.
51 C. W. Rella, K. D. Rector, A. S. Kwok, J. R. Hill, H. A. Schwettman, D. D. Dlott and M. D. Fayer, *J. Phys. Chem.*, 1996, **100**, 15620.
52 K. D. Rector, C. W. Rella, A. S. Kwok, J. R. Hill, S. G. Sligar, E. Y. P. Chien, D. D. Dlott and M. D. Fayer, *J. Phys. Chem. B*, 1997, **101**, 1468.
53 K. D. Rector, A. S. Kwok, C. Ferrante, R. S. Francis and M. D. Fayer, *Chem. Phys. Lett.*, 1997, **276**, 217.
54 K. D. Rector, D. Zimdars and M. D. Fayer, *J. Chem. Phys.*, 1998, **109**, 5455.
55 P. Hamm, M. Lim and R. M. Hochstrasser, *Phys. Rev. Lett.*, 1998, **81**, 5326.
56 P. Hamm, M. Lim, W. F. DeGrado and R. M. Hochstrasser, *J. Phys. Chem. A*, 1999, **103**, 10049.
57 M. C. Asplund, M. T. Zanni and R. M. Hochstrasser, *Proc. Natl. Acad. Sci. U. S. A.*, 2000, **97**, 8219.
58 K. A. Merchant, D. E. Thompson and M. D. Fayer, *Phys. Rev. Lett.*, 2001, **86**, 3899.
59 O. Golonzka, M. Khalil, N. Demirdöven and A. Tokmakoff, *Phys. Rev. Lett.*, 2001, **86**, 2154.
60 Y. Tanimura and S. Mukamel, *J. Chem. Phys.*, 1993, **99**, 9496.
61 V. Khidekel and S. Mukamel, *Chem. Phys. Lett.*, 1995, **240**, 304.
62 W. Zhao, V. Chernyak and S. Mukamel, *J. Chem. Phys.*, 1998, **110**, 5011.
63 K. Tominaga, G. P. Keogh, Y. Naitoh and K. Yoshihara, *J. Raman Spectrosc.*, 1995, **26**, 495.
64 (*a*) K. Tominaga and K. Yoshihara, *Phys. Rev. Lett.*, 1995, **74**, 3061; (*b*) K. Tominaga and K. Yoshihara, *Phys. Rev. Lett.*, 1996, **76**, 987; (*c*) K. Tominaga and K. Yoshihara, *J. Chem. Phys.*, 1996, **104**, 4419.
65 K. Okumura and Y. Tanimura, *J. Chem. Phys.*, 1997, **106**, 1687; 1997, **107**, 2267.
66 M. Cho, K. Okumura and Y. Tanimura, *J. Chem. Phys.*, 1997, **108**, 1326.
67 K. Okumra, A. Tokmakoff and Y. Tanimura, *J. Chem. Phys.*, 1999, **111**, 492.
68 A. Tokmakoff, M. J. Lang, D. S. Larsen, G. R. Fleming, V. Chernyak and S. Mukamel, *Phys. Rev. Lett.*, 1997, **79**, 2702.
69 A. Tokmakoff, M. J. Lang, X. J. Jordanides and G. R. Fleming, *Chem. Phys.*, 1998, **233**, 231.
70 T. Steffen and K. Duppen, *J. Chem. Phys.*, 1997, **106**, 3854; *Phys. Rev. Lett.*, 1996, **76**, 1224..
71 T. Steffen and K. Duppen, *Chem. Phys. Lett.*, 1997, **273**, 47.
72 T. Steffen, J. T. Fourkas and K. Duppen, *J. Chem. Phys.*, 1996, **105**, 7364.
73 M. Cho, Two-dimensional vibrational spectroscopy, in *Advances in Multi-photon Process and Spectroscopy*, ed. S. H. Lin, A. A. Villaeys and Y. Fujimura, World Scientific, Singapore, 1999, **vol. 12**, p. 229.
74 S. Hahn, K. Park and M. Cho, *J. Chem. Phys.*, 1999, **111**, 4121.
75 K. Park, S. Hahn and M. Cho, *J. Chem. Phys.*, 1999, **111**, 4131.
76 M. Cho, *J. Chem. Phys.*, 1999, **111**, 4140.
77 S. Hahn, K. Kwak and M. Cho, *J. Chem. Phys.*, 1999, **112**, 4553.
78 M. Cho, *J. Chem. Phys.*, 2000, **112**, 9978.
79 K. Park and M. Cho, *J. Chem. Phys.*, 2000, **112**, 10496.
80 D. Blank, L. Kaufman and G. R. Fleming, *J. Chem. Phys.*, 1999, **111**, 3105.
81 D. J. Ulness, J. C. Kirkwood and A. C. Albrecht, *J. Chem. Phys.*, 1998, **108**, 3897.
82 J. C. Kirkwood, D. J. Ulness, A. C. Albrecht and M. J. Stimson, *Chem. Phys. Lett.*, 1998, **293**, 417.
83 L. J. Kaufman, J. Heo, G. R. Fleming, J. Sung and M. Cho, *Chem. Phys.*, 2001, **266**, 251.
84 K. Park and M. Cho, *J. Chem. Phys.*, 1998, **109**, 10559.
85 M. Cho, *Phys. Rev. A*, 2000, **61**, 23406.
86 M. Cho, *J. Chem. Phys.*, 1998, **109**, 5327.
87 D. Blank, L. Kaufman and G. R. Fleming, *J. Chem. Phys.*, 2000, **113**, 771.
88 (*a*) L. Kaufman, D. Blank and G. R. Fleming, *J. Chem. Phys.*, 2001, **114**, 2312; (*b*) L. Kaufman, J. Heo, L. D. Ziegler and G. R. Fleming, *Phys. Rev. Lett.*, 2001, submitted.
89 W. Zhao and J. C. Wright, *Phys. Rev. Lett.*, 1999, **83**, 1950.
90 W. Zhao and J. C. Wright, *J. Am. Chem. Soc.*, 1999, **121**, 10994; W. Zhao and J. C. Wright, *Phys. Rev. Lett.*, 2000, **84**, 1411.
91 M. Bonn, Ch. Hess, J. H. Miners, H. J. Bakker, T. F. Heinz and M. Cho, *Phys. Rev. Lett.*, 2001, **86**, 1566.
92 P. Hamm, M. Lim and R. Hochstrasser, *J. Chem. Phys.*, 2000, **112**, 1907.
93 J. Sung and M. Cho, *J. Chem. Phys.*, 2000, **113**, 7072.
94 J. Sung, R. J. Silbey and M. Cho, *J. Chen. Phys.*, 2001, **115**, 1422.

95 K. Okumura, D. M. Jonas and Y. Tanimura, *Chem. Phys.*, 2001, **266**, 237.
96 K. Park and M. Cho, *J. Chem. Phys.*, 2000, **112**, 5021.
97 (*a*) S. Saito and I. Ohmine, *J. Chem. Phys.*, 1998, **108**, 24–251; (*b*) S. Saito and I. Ohmine, *Phys. Rev. Lett.*, 2001.
98 R. L. Murry, J. T. Fourkas and T. Keyes, *J. Chem. Phys.*, 1998, **109**, 2814–25.
99 R. L. Murry and J. T. Fourkas, *J. Chem. Phys.*, 1997, **107**, 9726–40.
100 A. Ma and R. M. Stratt, *Phys. Rev. Lett.*, 2000, **85**, 1004.
101 R. A. Denny and D. R. Reichman, *Phys. Rev. E*, 2001, **63**, 63.
102 (*a*) T. I. C. Jansen, J. G. Snijders and K. Duppen, *J. Chem. Phys.*, 2000, **113**, 307; (*b*) T. I. C. Jansen, J. G. Snijders and K. Duppen, *J. Chem. Phys.*, 2001, **114**, 10910.
103 S. Krimm and J. Bandekar, *Adv. Protein Chem.*, 1986, **38**, 181 and references therein.
104 H. Torii and M. Tasumi, *J Chem. Phys.*, 1992, **96**, 3379.
105 *Infrared and Raman Spectroscopy of Biological Materials*, ed. H.-U. Gremlich and B. Yan, Marcel Dekker, Inc., New York, 2000.
106 R. Ernst, G. Bodenhausen and A. Wokaun, *Principles of Nuclear Magnetic Resonance in One and Two Dimensions*, Clarendon, Oxford, 1987.
107 J. K. M. Sanders and B. K. Hunter, *Modern NMR Spectroscopy; A Guide for chemists* (Oxford University Press, New York, 1994.
108 M. Cho, *J. Chem. Phys.*, 2002, **116**, 1562.
109 S. Ruhman, A. G. Joly and K. A. Nelson, *IEEE J. Quantum Electron.*, 1988, **24**, 460.
110 D. McMorrow, N. Thantu, J. S. Melinger, S. K. Kim and W. T. Lotshaw, *J. Phys. Chem.*, 1996, **100**, 10389–99.
111 W. T. Lotshaw, D. McMorrow, N. Thantu, J. S. Melinger and R. Kitchenham, *J. Raman Spectrosc.*, 1995, **26**, 571–83.
112 D. McMorrow, W. T. Lotshaw and G. A. Kenney-Wallace, *IEEE J. Quantum Electron.*, 1988, **QE-24**, 443.
113 Y. J. Chang and E. W. Castner Jr., *J. Chem. Phys.*, 1994, **98**, 12600.
114 R. A. Farrer, B. J. Loughnane, L. A. Deschenes and J. T. Fourkas, *J. Chem. Phys.*, 1997, **106**, 6901.
115 T. Hattori and T. Kobayashi, *J. Chem. Phys.*, 1991, **94**, 3332.
116 P. Vohringer and N. F. Scherer, *J. Chem. Phys.*, 1995, **99**, 2684.
117 G. D. Goodno and R. J. D. Miller, *J. Phys. Chem. A*, 1999, **103**, 10619.
118 M. Cho, M. Du, N. F. Scherer, G. R. Fleming and S. Mukamel, *J. Chem. Phys.*, 1993, **99**, 2410.
119 M. Khalil, O. Golonzka, N. Demirdöven, C. J. Fecko and A. Tokmakoff, *Chem. Phys. Lett.*, 2000, **321**, 231.
120 N. A. Smith and S. R. Meech, *Faraday Discuss.*, 1997, **108**, 35.
121 M. Cho, *J. Chem. Phys.*, 2001, **114**, 9982.
122 E. Yablonovitch, C. Flytzanis and N. Bloembergen, *Phys. Rev. Lett.*, 1972, **29**, 865.
123 I. Chabay, G. K. Klauminzer and B. S. Hudson, *Appl. Phys. Lett.*, 1976, **28**, 27.
124 J. E. Ivanecky, III and J. C. Wright, *Chem. Phys. Lett.*, 1993, **206**, 437.
125 D. J. Ulness, J. C. Kirkwood and A. C. Albrecht, *J. Chem. Phys.*, 1998, **108**, 3897.
126 J. C. Kirkwood, D. J. Ulness, A. C. Albrecht and M. J. Stimson, *Chem. Phys. Lett.*, 1998, **293**, 417.
127 D. A. Blank, L. J. Kaufman and G. R. Fleming, *J. Chem. Phys.*, 1999, **111**, 3105.
128 D. A. Blank, G. R. Fleming, M. Cho and A. Tokmakoff, in *Ultrafast Infrared and Raman Spectroscopy*, ed. M. D. Fayer, Marcel Dekker, Inc., New York, 2000.
129 M. Cho, D. A. Blank, J. Sung, K. Park, S. Hahn and G. R. Fleming, *J. Chem. Phys.*, 2000, **112**, 2082.
130 M. J. Labuda and J. C. Wright, *J. Chem. Phys.*, 1998, **108**, 4112.
131 D. M. Besemann, N. J. Condon, K. M. Murdoch, W. Zhao, K. A. Meyer and J. C. Wright, *Chem. Phys.*, 2001, **266**, 177.
132 M. Cho, *J. Chem. Phys.*, 2001, **115**, 4424.
133 R. Kubo, *Adv. Chem. Phys.*, 1963, **13**, 101.
134 S. Mukamel, *Principles of Nonlinear Optical Spectroscopy*, Oxford University Press, London, 1995.
135 I. Noda, *J. Am. Chem. Soc.*, 1989, **111**, 8116.
136 I. Noda, *Appl. Spectrosc.*, 1990, **44**, 550.
137 *Two-Dimensional Correlation Spectroscopy*, ed. Y. Ozaki and I. Noda, AIP Conference Proceedings, vol. 503, American Institute of Physics, New York,1999.
138 G. R. Fleming and M. Cho, *Ann. Rev. Phys. Chem.*, 1996, **47**, 103.
139 D. A. Wiersma, W. P. de Boeij and M. S. Pshenichnikov, *Ann. Rev. Phys. Chem.*, 1998, **49**, 99.
140 M. Cho and G. R. Fleming, *Adv. Chem. Phys.*, ed. J. Jortner and M. Bixon, Wiley, New York, 1999, vol. 107, Part II, pp. 311–370.
141 R. M. Stratt and M. Cho, *J. Chem. Phys.*, 1994, **100**, 6700.
142 B. M. Ladanyi and S. Klein, *J. Chem. Phys.*, 1996, **105**, 1552.
143 G. M. Gale, G. Gallot, F. Hache, N. Lascoux, S. Bratos and J.-Cl. Leicknam, *Phys. Rev. Lett.*, 1999, **82**, 1068.
144 S. Bratos, G. M. Gale, G. Gallot, F. Hache, N. Lascoux and J.-Cl. Leicknam, *Phys. Rev. E*, 2000, **61**, 5211.
145 H.-K. Nienhuys, S. Woutersen, R. A. van Santen and H. J. Bakker, *J. Chem. Phys.*, 1999, **111**, 1494.
146 S. Woutersen and P. Hamm, *J. Phys. Chem. B*, 2000, **104**, 11316.
147 S. Woutersen and P. Hamm, *J. Chem. Phys.*, 2001, **114**, 2727.
148 A. Piryatinski, V. Chernyak and S. Mukamel, in *Ultrafast Infrared and Raman Spectroscopy*, ed. M. D. Fayer, Marcel Dekker Inc., New York, 2001.
149 W. H. Hesselink and D. A. Wiersma, *Phys. Rev. Lett.*, 1979, **43**, 1991; *J. Chem. Phys.*, 1980, **73**, 648..
150 P. C. Becker, H. L. Fragnito, J.-Y. Bigot, C. Brito-Cruz, R. L. Fork and C. V. Shank, *Phys. Rev. Lett.*, 1989, **63**, 505; J.-Y. Bigot, M. T. Portella, R. W. Schoenlein, C. J. Bardeen, A. Migus and C. V. Shank, *Phys. Rev. Lett.*, 1991, **66**, 1138.
151 T. Joo and A. C. Albrecht, *Chem. Phys.*, 1993, **176**, 233.
152 P. Vohringer, D. C. Arnett, T.-S. Yang and N. F. Scherer, *Chem. Phys. Lett.*, 1995, **237**, 387.
153 M. Cho, J.-Y. Yu, T. Joo, Y. Nagasawa, S. A. Passino and G. R. Fleming, *J. Phys. Chem.*, 1996, **100**, 11944.
154 M. T. Zanni, S. Gnanakaran, J. Stenger and R. M. Hochstrasser, *J. Phys. Chem. B*, 2001, **105**, 6520.
155 D. E. Thompson, K. A. Merchant and M. D. Fayer, *J. Chem. Phys.*, 2001, **115**, 317.
156 M. Cho, *J. Chem. Phys.*, 1997, **106**, 7550.
157 R. F. Loring and S. Mukamel, *J. Chem. Phys.*, 1985, **83**, 2119.
158 D. A. V. Bout, L. J. Muller and M. Berg, *Phys. Rev. Lett.*, 1991, **67**, 3700.
159 M. Berg and D. A. V. Bout, *Acc. Chem. Res.*, 1997, **30**, 65.
160 D. A. V. Bout and M. Berg, *J. Raman Spectrosc.*, 1995, **26**, 503.
161 L. J. Muller, D. A. V. Bout and M. Berg, *J. Chem. Phys.*, 1993, **99**, 810.
162 R. Inaba, K. Tominaga, K. Tasumi and K. A. Nelson, *Chem. Phys. Lett.*, 1993, **211**, 183.
163 X. D. Zhu, H. Suhr and Y. R. Shen, *Phys. Rev. B*, 1987, **35**, 3047.
164 P. Guyot-Sionnest, J. H. Hunt and Y. R. Shen, *Phys. Rev. Lett.*, 1987, **59**, 1597.
165 R. Superfine, J. Y. Huang and Y. R. Shen, *Phys. Rev. Lett.*, 1991, **66**, 1066.
166 Y. R. Shen, *Surf. Sci.*, 1994, **299**(300), 551.
167 S. H. Lin and A. A. Villaeys, *Phys. Rev. A*, 1994, **50**, 5134.
168 Y. R. Shen, *Nature*, 1989, **337**, 519 and references therein.
169 T. Kato, M. Hayashi, A. A. Villaeys and S. H. Lin, *Phys. Rev. A*, 1997, **56**, 980.
170 T. F. Heinz, F. J. Himpsel, E. Palange and E. Burstein, *Phys. Rev. Lett.*, 1989, **63**, 644.
171 M. Y. Jiang, G. Pajer and E. Burstein, *Surf. Sci.*, 1991, **242**, 306.
172 Y. J. Chabal, *Surf. Sci. Rep.*, 1988, **8**, 211.
173 E. J. Heilweil, M. P. Casassa, R. R. Cavanagh and J. C. Stephenson, *Annu. Rev. Phys. Chem.*, 1989, **40**, 143.
174 A. L. Harris and N. J. Levinos, *J. Chem. Phys.*, 1989, **90**, 3878.
175 A. L. Harris, L. Rothberg, L. H. Dubois, N. J. Levinos and L. Dhar, *Phys. Rev. Lett.*, 1990, **64**, 2086; A. L. Harris and L. Rothberg, *J. Chem. Phys.*, 1991, **94**, 2449.
176 M. Morin, N. J. Levinos and A. L. Harris, *J. Chem. Phys.*, 1992, **96**, 3950.
177 K. Kuhnke, M. Morin, P. Jakob, N. L. Levinos, Y. J. Chabal and A. L. Harris, *J. Chem. Phys.*, 1993, **99**, 6114.
178 A. Peremans and A. Tadjeddine, *Phys. Rev. Lett.*, 1994, **73**, 3010; A. Peremans, A. Tadjeddine and P. Guyot-Sionnest, *Chem. Phys. Lett.*, 1995, **247**, 243.
179 J. D. Beckerle, R. R. Cavanagh, M. P. Casassa, E. J. Heilweil and J. C. Stephenson, *J. Chem. Phys.*, 1991, **95**, 5403.
180 P. Guyot-Sionnest, P. Dumas, Y. J. Chabal and G. H. Higashi, *Phys. Rev. Lett*, 1990, **64**, 2156.
181 C. Matranga and P. Guyot-Sionnest, *J. Chem. Phys.*, 2000, **112**, 7615.
182 R. P. Chin, J. Y. Huang, Y. R. Shen, T. J. Chuang, H. Seki and M. Buck, *Phys. Rev. Lett.*, 1992, **45**, 1522.
183 D. E. Gragson and G. L. Richmond, *J. Chem. Phys.*, 1997, **107**, 9687.
184 S. Baldelli, C. Schnitzer and M. J. Shultz, *J. Chem. Phys.*, 1998, **108**, 9817.
185 M. E. Schmidt and P. Guyot-Sionnest, *J. Chem. Phys.*, 1996, **104**, 2438.

186 M. Bonn, Ch. Hess, S. Funk, J. H. Miners, B. N. J. Persson, M. Wolf and G. Ertl, *Phys. Rev. Lett.*, 2000, **84**, 4653.
187 M. Cho, Ch. Hess and M. Bonn, 2002, submitted.
188 P. Guyot-Sionnest, *Phys. Rev. Lett.*, 1991, **66**, 1489.
189 M. A. Belkin, T. A. Kulakov, K.-H. Ernst, L. Yan and Y. R. Shen, *Phys. Rev. Lett.*, 2000, **85**, 4474.
190 F. Liu, *J. Phys. Chem.*, 1991, **95**, 7180.
191 M. Gruebele, J. Sabelko, R. Ballew and J. Ervin, *Acc. Chem. Res.*, 1998, **31**, 699.
192 M. Cho, *J. Chem. Phys.*, 2001, **114**, 8040.
193 M. Cho, *J. Chem. Phys.*, 2000, **113**, 7746.
194 M. Cho, *J. Chem. Phys.*, 1999, **111**, 10587.
195 H. A. Kramers, *Physica*, 1940, **7**, 284.
196 R. F. Grote and J. T. Hynes, *J. Chem. Phys.*, 1980, **73**, 2715; 1981, **74**, 4465.
197 P. Hänggi, P. Talkner and M. Borkovec, *Rev. Mod. Phys.*, 1990, **62**, 250.
198 *Activated Barrier Crossing; Applications in Physics, Chemistry, and Biology*, ed. G. R. Fleming and P. Hänggi, World Scientific, Singapore, 1993.
199 B. Bagchi and A. Chandra, *Adv. Chem. Phys.*, 1991, **80**, 1.
200 F. O. Raineri, H. Resat, B.-C. Perng, F. Hirata and H. L. Friedman, *J. Chem. Phys.*, 1994, **100**, 1477.
201 P. V. Kumar and M. Maroncelli, *J. Chem. Phys.*, 1995, **103**, 3038.
202 R. M. Stratt and M. Cho, *J. Chem. Phys.*, 1994, **100**, 6700.
203 R. M. Stratt and M. Maroncelli, *J. Phys. Chem.*, 1996, **100**, 12981.
204 B. M. Ladanyi and R. M. Stratt, *J. Phys. Chem.*, 1995, **99**, 2502.
205 M. Cho and G. R. Fleming, *J. Phys. Chem.*, 1994, **98**, 3478.